Thermodynamics, density profiles, and correlation functions of the inhomogeneous one-dimensional spinor Bose gas

Ovidiu I. Pâţu[1] and Andreas Klümper[2]
[1]*Institute for Space Sciences, Bucharest-Măgurele, R 077125, Romania*
[2]*Fachbereich C Physik, Bergische Universität Wuppertal, 42097 Wuppertal, Germany*
(Received 1 September 2015; published 29 October 2015)

We investigate the finite-temperature properties of the one-dimensional two-component Bose gas (2CBG) with repulsive contact interaction in a harmonic trap. Making use of a lattice embedding for the 2CBG and the quantum transfer matrix, we derive a system of two nonlinear integral equations characterizing the thermodynamics of the uniform system for all values of the relevant parameters: temperature, strength of the interaction, chemical potential, and magnetic field. This system allows for an easy numerical implementation in stark contrast with the infinite number of equations obtained by employing the thermodynamic Bethe ansatz. We use this exact solution coupled with the local density approximation to compute the density profiles and local density correlation function of the inhomogeneous gas for a wide range of coupling strengths and temperatures. Our results show that the polarization in the center of the trap influences heavily the local correlator especially in the experimentally accessible Tonks-Girardeau regime.

DOI: 10.1103/PhysRevA.92.043631 PACS number(s): 67.85.−d, 02.30.Ik

I. INTRODUCTION

As a result of the growing expertise in the creation and the manipulation of ultracold atomic gases, we have witnessed in recent years the experimental realization of various strongly interacting many-body systems characterized by an extreme degree of purity and excellent control of relevant parameters including temperature, strength of the interaction, and even dimensionality [1–3]. In particular, one-dimensional (1D) gases which can be created using optical lattices or atom chips are extremely interesting for several reasons. One reason is that these systems exhibit regimes such as the Luttinger liquid (LL) [4], spin-incoherent LL [5–7], and the ferromagnetic liquid [8–11], which are not present in 2D and 3D. In addition, the high degree of control of the relevant parameters means that some of these systems can be well approximated by integrable systems providing a parameter-free comparison of theoretical predictions with measurements. The paradigmatic example in this case is the experimental realization [12–17] of the Lieb-Liniger model [18] which has been investigated theoretically for more than 50 years.

It is natural to expect that one-dimensional physical systems comprised of particles with internal degrees of freedom present a wider range of phenomena than their single-component counterparts. Such spinor gases have been produced [19–25] by trapping atoms in two or more internal states which can be referred as (pseudo)spin states. In the case of fermionic spinor gases, the ground state is antiferromagnetic [26] and at low energy they are described by the LL theory. In addition, the phenomenon of spin-charge separation is present which means that the Hilbert space separates in two independent sectors: one for the collective spin excitations and one for the collective charge excitations. The situation involving bosonic spinor gases is more complex. While there are cases in which the physics is similar to their fermionic counterpart [27], in the case of spin-independent interactions, which is integrable and will be the main subject of this paper, the ground state is ferromagnetic [28,29]. The spin excitations have a dispersion behaving like k^2 which makes the application of the LL theory impossible. For these systems, the low-energy sector is described by a universality class called the ferromagnetic liquid [8–11].

In this article, we are going to investigate the thermodynamics, density profiles, and local density-density correlation function of the trapped 1D two-component Bose gas interacting via a δ-function potential using the exact solution of the uniform system and the local density approximation (LDA). From the historical point of view, the first exact solution of an integrable multicomponent system was obtained by Yang [30] and Gaudin [31] for the two-component fermionic case using what we call nowadays the nested Bethe ansatz. The spectrum of the two-component Bose gas (2CBG) was derived in [32,33] and the low-lying excitations were investigated in [33]. The spin-wave excitations, spin dynamics, edge exponent in the dynamic spin structure factor, ground-state properties in a trap at $T = 0$, and impurity dynamics can be found in [34–44]. Even though the study of nonlocal correlation functions is still in its early stages [45,46], recent progress in the calculation of form factors [47–49] opens the way for the calculation of correlators along the lines of [50,51]. As a result of the integrability of the model one might believe that computing the thermodynamical properties should be an accessible task. Unfortunately, this assertion is not true. For example, the application of the thermodynamical Bethe ansatz (TBA) [52,53] produces an infinite number of nonlinear integral equations (NLIEs) [54] which makes the extraction of physical information extremely difficult. Even though some important results can be derived on the basis of the TBA equations [55–57], it is highly desirable to obtain an alternative thermodynamic description allowing for an easy numerical implementation. Our result, Eqs. (6) and (7), which was derived using the quantum transfer matrix (QTM) and a lattice embedding of the 2CBG, provides such an alternative description.

The basis of our method is the following observation. Consider an integrable continuum model and one of its lattice embeddings. By lattice embedding of a continuum model we understand an integrable model defined on a lattice whose

 ©2015 American Physical Society

Bethe equations and spectrum transform in a specific scaling limit in the Bethe equations and spectrum of the continuum model. Then, the thermodynamics of the continuum model can be derived from the thermodynamics of the lattice model if we perform the same scaling limit as in the case of the Bethe equations and spectrum. One example is the Yang-Yang thermodynamics [52] of the Lieb-Liniger model which was obtained from the thermodynamics of the critical XXZ spin chain [58]. As we will show in Sec. IV, in the case of the 2CBG the relevant lattice model is the critical $q = 3$ Perk-Schultz spin chain [59–64]. The thermodynamics of the spin chain is derived using the quantum transfer matrix method [65–69], which can be defined only for lattice models but has the fundamental advantage of providing a finite number of integral equations. Performing the scaling limit in these equations, we obtain Eqs. (6) and (7). This finite system of equations coupled with the LDA allows for the calculation of the density profiles and the local density-density correlation function of the system subjected to a slowly varying harmonic potential.

The plan of the paper is as follows. In Sec. II, we introduce the 2CBG and the thermodynamic description of the uniform system. The results for the density profiles and local correlator are presented in Sec. III. Section IV contains the lattice embedding of the 2CBG and in Sec. V we remind some notions of the algebraic Bethe ansatz and introduce the quantum transfer matrix. The derivation of the free energy of the spin chain can be found in Sec. VI and the continuum limit is performed in Sec. VII. The nested Bethe ansatz solution of the generalized $q = 3$ Perk-Schultz model and the proof of several useful identities can be found in Appendices A and B. Some of the results presented in this article were announced in the short paper [70].

II. ONE-DIMENSIONAL TWO-COMPONENT BOSE GAS

We consider a one-dimensional system of equal mass bosons with two internal degrees of freedom interacting via a δ-function potential and constrained on a ring of circumference L_B (periodic boundary conditions). The second quantized Hamiltonian in the presence of a harmonic trapping potential $V(x) = m\omega x^2/2$ is

$$\mathcal{H}_{\text{Bose}} = \int_0^{L_B} dx \left\{ \frac{\hbar^2}{2m}(\partial_x \Psi^\dagger \partial_x \Psi) + \frac{g}{2} :(\Psi^\dagger\Psi)^2: + [V(x) - \mu](\Psi^\dagger\Psi) - H(\Psi^\dagger\sigma_z\Psi) \right\}, \tag{1}$$

with $\Psi = \binom{\Psi_1(x)}{\Psi_2(x)}$, $\Psi^\dagger = (\Psi_1^\dagger(x) \quad \Psi_2^\dagger(x))$, $\sigma_z = \begin{pmatrix} 1 & 0 \\ 0 & -1 \end{pmatrix}$, where $\Psi_a(x)$, $a = \{1,2\}$, are 1D quantum fields satisfying canonical commutation relations $\Psi_a(x)\Psi_b^\dagger(y) - \Psi_b^\dagger(y)\Psi_a(x) = \delta_{ab}\delta(x-y)$. In (1), $g > 0$ is the coupling constant, μ is the chemical potential, H the external magnetic field (the Bohr magneton and the Lande factors are absorbed into H), ω is the trap oscillation frequency, m is the mass of the particles, and $:\ldots:$ denotes normal ordering. In experiments, the internal degrees of freedom are two distinguishable hyperfine states which can be thought of as a (pseudo)spin $\frac{1}{2}$. Compared with the scalar case (Lieb-Liniger model [18]), the wave functions of the 2CBG are symmetric only under exchange of coordinates of particles with the same spin. One-dimensional systems that are well approximated by the Hamiltonian (1) can be experimentally achieved in highly elongated cylindrical traps ($\omega \ll \omega_\perp$) where $\omega_\perp$ is the trap oscillation frequency in the transversal plane. Assuming that the 3D scattering length $a_{3\text{D}}$ is much smaller than the transverse harmonic oscillator length $l_\perp = \sqrt{\hbar/m\omega_\perp}$, the coupling strength can be expressed as $g \simeq 2\hbar^2 a_{3\text{D}}/(m l_\perp^2) = 2\hbar\omega_\perp a_{3\text{D}}$ [71,72]. The realization of the 1D regime requires that $\hbar\omega_\perp$ is larger than the thermal energy $k_B T$ and the chemical potential μ [73,74]. The experimental advances of the last decade paved the way for the experimental realization of such quasi-1D systems [1–3] characterized by coupling strengths which range from weak coupling ($\gamma \ll 1$) to the strongly interacting Tonks-Girardeau regime ($\gamma \gg 1$). In order to lighten the notation in the following, we are going to consider $\hbar = k_B = 2m = 1$ and introduce the effective interaction parameter $c = gm/\hbar^2$.

A. Bethe-ansatz solution for the uniform system

Even though the Hamiltonian (1) is integrable only when the system is homogeneous [$V(x) = 0$], the trapped system can be efficiently investigated using the solution of the uniform system coupled with the local density approximation. Therefore, we will first review the exact solution of the homogeneous 2CBG and defer the treatment of the inhomogeneous system to Sec. III. Since we are interested in investigating the thermodynamic behavior, we will consider only the case of repulsive interaction $c > 0$ (for $c < 0$ the system is thermodynamically unstable). For a system of M particles of which M_1^B are of type 1 and M_2^B are of type 2 ($M = M_1^B + M_2^B$), the energy spectrum of the 2CBG obtained using the nested Bethe ansatz [32,33] (see also Refs. [75–77]) is

$$E_{\text{Bose}} = \sum_{j=1}^{M} \bar{e}_0\big(k_j^{(1)}\big) - H\big(M_1^B - M_2^B\big), \quad \bar{e}_0(k) = k^2 - \mu, \tag{2}$$

with $\{k_j^{(1)}\}$ satisfying the Bethe-ansatz equations (BAEs)

$$e^{ik_s^{(1)}L_B} = \prod_{\substack{j=1\\ j\neq s}}^{M} \frac{k_s^{(1)} - k_j^{(1)} + ic}{k_s^{(1)} - k_j^{(1)} - ic} \prod_{p=1}^{M_1^B} \frac{k_s^{(1)} - k_p^{(2)} - ic/2}{k_s^{(1)} - k_p^{(2)} + ic/2}, \quad s = 1,\ldots,M \tag{3a}$$

$$\prod_{j=1}^{M} \frac{k_l^{(2)} - k_j^{(1)} + ic/2}{k_l^{(2)} - k_j^{(1)} - ic/2} = \prod_{\substack{p=1\\ p\neq l}}^{M_1^B} \frac{k_l^{(2)} - k_p^{(2)} + ic}{k_l^{(2)} - k_p^{(2)} - ic}, \quad l = 1,\ldots,M_1^B. \tag{3b}$$

The solution is characterized by two sets of rapidities $\{k_j^{(1)}\},\{k_j^{(2)}\}$ (a general characteristic of integrable two-component systems) with the second set of rapidities contributing to the energy (2) only via the BAEs.

Even in the case of integrable models, computing the thermodynamics is an extremely challenging task. One way to tackle this problem is the utilization of the thermodynamic Bethe ansatz [52,53]. In this framework, the grand-canonical potential of the system is ($\beta = 1/T$) [54]

$$\phi(\mu,H,\beta) = -\frac{1}{2\pi\beta}\int_{-\infty}^{+\infty} dk\ \ln[1+\eta_1(k)], \tag{4}$$

with $\eta_1(k)$ satisfying the following infinite system of nonlinear integral equations:[1]

$$\ln\eta_1(k) = -\beta(k^2-\mu-H) + a_3 * f * \ln[1+\eta_1(k)] + f * \ln[1+\eta_2(k)], \tag{5a}$$

$$\ln\eta_n(k) = f * \{\ln[1+\eta_{n-1}(k)] + \ln[1+\eta_{n+1}(k)]\}, \quad n = 2,\ldots,\infty \tag{5b}$$

together with the asymptotic condition $\lim_{n\to\infty}\ln\eta_n(k)/n = 2\beta H$. In Eqs. (5), $g * h(k) \equiv \int_{-\infty}^{+\infty} g(k-k')h(k')\ dk'$, $f(k) = 1/[2c\cosh(\pi k/c)]$, and $a_n(k) = nc/\{2\pi[(nc/2)^2 + k^2]\}$. While important, it is obvious that extracting physically relevant information from this system of equations is very hard even from the numerical point of view (see Refs. [55–57]), highlighting the need for a more manageable thermodynamic description of the 2CBG which will be presented in the next section.

B. Alternative thermodynamic description of the uniform 2CBG

A more efficient thermodynamic description of the 2CBG was proposed in [70]. The full derivation of this result which is based on the connection of our model with the $(---)$ Perk-Schultz spin chain and the quantum transfer matrix method represents one of the main results of this paper and will be presented in Secs. VI and VII. In this description, the grand-canonical potential per unit length of the 2CBG is

$$\phi(\mu,H,\beta) = -\frac{1}{2\pi\beta}\int_{\mathbb{R}}\{\ln[1+a_1(k)] + \ln[1+a_2(k)]\}dk, \tag{6}$$

with $a_{1,2}(k)$ auxiliary functions satisfying the following system of integral equations:

$$\ln a_1(k) = -\beta(k^2-\mu-H) + \int_{\mathbb{R}} K_0^B(k-k')\ln[1+a_1(k')]\,dk' + \int_{\mathbb{R}} K_2^B(k-k'-i\varepsilon)\ln[1+a_2(k')]\,dk', \tag{7a}$$

$$\ln a_2(k) = -\beta(k^2-\mu+H) + \int_{\mathbb{R}} K_1^B(k-k'+i\varepsilon)\ln[1+a_1(k')]\,dk' + \int_{\mathbb{R}} K_0^B(k-k')\ln[1+a_2(k')]\,dk', \tag{7b}$$

where $\varepsilon \to 0$ and

$$K_0^B(k) = \frac{1}{2\pi}\frac{2c}{k^2+c^2}, \quad K_1^B(k) = \frac{1}{2\pi}\frac{c}{k(k+ic)}, \quad K_2^B(k) = \frac{1}{2\pi}\frac{c}{k(k-ic)}. \tag{8}$$

We can check the validity of our result in three well-known limits. First, we will address the noninteracting limit $c \to 0$. Using $\lim_{c\to 0} K_2^B(k-i\varepsilon) = \lim_{c\to 0} K_1^B(k+i\varepsilon) = 0$ and $\lim_{c\to 0} K_0^B(k-k') = \delta(k-k')$, the NLIEs (7) decouple with the result

$$\ln a_1(k) = -\beta(k^2-\mu-H) + \ln[1+a_1(k)],$$
$$\ln a_2(k) = -\beta(k^2-\mu+H) + \ln[1+a_2(k)].$$

These equations are easily solved obtaining

$$\phi(\mu,H,\beta) = \frac{1}{2\pi\beta}\int_{\mathbb{R}}[\ln(1-e^{-\beta(k^2-\mu-H)}) + \ln(1-e^{-\beta(k^2-\mu+H)})]dk,$$

which is exactly the grand-canonical potential of two noninteracting Bose gases at different chemical potentials.

In the strong magnetic field limit $H \to \infty$, due to the fact that the inhomogeneity $-\beta(k^2-\mu+H)$ is large and negative $a_2(k) \sim 0$, which means that the thermodynamics of the system is given by

$$\phi(\mu,H,\beta) = -\frac{1}{2\pi\beta}\int_{\mathbb{R}}\ln[1+a_1(k)]\,dk,$$
$$\ln a_1(k) = -\beta(k^2-\mu-H) + \int_{\mathbb{R}} K_0^B(k-k') \times \ln[1+a_1(k')]\,dk'.$$

This result, which is the Yang-Yang thermodynamics [52] of the Lieb-Liniger gas, confirms the natural expectation that in the strong magnetic limit the system will become fully polarized, and, therefore, the thermodynamics will be the same as in the single-component case. In a similar fashion, we can show that if the magnetic field is fixed and finite, then, in the low-temperature limit ($T \ll \mu,H,c$), the same formulas are obtained proving that the ground state is ferromagnetic (fully polarized).

In the limit of impenetrable particles $c \to \infty$, the system is effectively "fermionized" and we should reproduce the result obtained by Takahashi (Chap. 12 of [53]) for impenetrable repulsive two-component fermions (2CFG)

$$\phi_F(\mu,H,\beta) = -\frac{1}{2\pi\beta}\int_{\mathbb{R}} dk\ \ln[1+2\cosh(\beta H)e^{-\beta(k^2-\mu)}]. \tag{9}$$

[1]This form of the TBA equations can be easily derived from the one used in [56,57] by the use of simple transformations and identities as in Chap. 12 of [53].

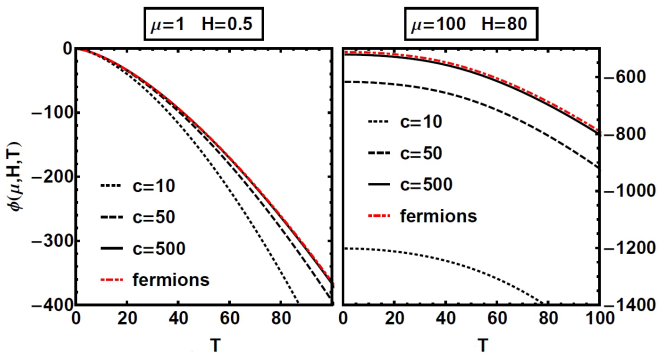

FIG. 1. (Color online) Plot of the grand-canonical potential per length of the 2CBG and impenetrable 2CFG (dotted-dashed line) as a function of temperature for $\mu = 1\,, H = 0.5$ (left panel) and $\mu = 100\,, H = 80$ (right panel). For large values of the coupling constant, the 2CBG result approaches asymptotically Eq. (9). Grand-canonical potential per length, temperature, chemical potential, and magnetic field in units of ϕ_0, T_0, μ_0, and h_0 [78].

Even though we did not succeed in providing an analytic proof of this equivalence, we have checked numerically and found perfect agreement as can be seen in Fig. 1.

C. "Heuristic" derivation

The rigorous and self-contained derivation of the thermodynamic description presented in the previous section will be given in Secs. VI and VII. Here, we provide a heuristic derivation based on the fact that the system of equations (5) share the same structure with the NLIEs for the spin-$\frac{1}{2}$ XXX spin chain. Let us be more precise. We consider a very general XXX spin chain case characterized by the Hamiltonian $\mathcal{H}_{XXX} = \mathcal{H}_0 + \sum_n \beta_n \mathcal{J}_n$ with nearest-neighbor interaction $\mathcal{H}_0$ and higher conserved currents $\mathcal{J}_n$. Explicitly, we have $\mathcal{H}_0 := J \sum_i (2\vec{S}_i \vec{S}_{i+1} + \frac{1}{2}) - \tilde{H} \sum_i S_i^z$, with J and $\tilde{H}$ the interaction strength and magnetic field. The TBA result for the free energy per unit length is $F(\tilde{H},\beta) = \tilde{e}_0 - \beta^{-1} \int_{-\infty}^{+\infty} dk\, f(k) \ln[1 + \tilde{\eta}_1(k)]$ $\{\tilde{e}_0$ is the zero-point energy and $f(k) = 1/[2\cosh(\pi k)]$, $\tilde{f} = f + \sum_n \beta_n f^{(n)}\}$ with $\tilde{\eta}_1(k)$ satisfying

$$\ln \tilde{\eta}_1(k) = -2\pi\beta J \tilde{f}(k) + f * \ln[1 + \tilde{\eta}_2(k)], \tag{10a}$$

$$\ln \tilde{\eta}_n(k) = f * \{\ln[1 + \tilde{\eta}_{n-1}(k)] + \ln[1 + \tilde{\eta}_{n+1}(k)]\}, \quad n = 2, \ldots, \infty \tag{10b}$$

together with the asymptotic condition $\lim_{n\to\infty} \ln \tilde{\eta}_n(k)/n = \beta\tilde{H}$. A more compact result can be obtained using the quantum transfer matrix [68,69,79] yielding $F(\tilde{H},\beta) = \tilde{e}_0 - \beta^{-1} \int_{-\infty}^{+\infty} dk\, f(k)\{\ln[1 + \tilde{a}_1(k)] + \ln[1 + \tilde{a}_2(k)]\}$, with only two auxiliary functions satisfying

$$\ln \tilde{a}_1(k) = -\beta[2\pi J \tilde{f}(k) - \tilde{H}/2] + \tilde{K}_0 * \ln[1 + \tilde{a}_1(k)] - \tilde{K}_2 * \ln[1 + \tilde{a}_2(k)], \tag{11a}$$

$$\ln \tilde{a}_2(k) = -\beta[2\pi J \tilde{f}(k) + \tilde{H}/2] - \tilde{K}_1 * \ln[1 + \tilde{a}_1(k)] + \tilde{K}_0 * \ln[1 + \tilde{a}_2(k)], \tag{11b}$$

where

$$\tilde{K}_0(k) = \frac{1}{2\pi} \int_{-\infty}^{+\infty} \frac{e^{ikx} e^{-|x|/2}}{2\cosh\frac{x}{2}}\, dx,$$

$$\tilde{K}_1(k) = \frac{1}{2\pi} \int_{-\infty}^{+\infty} \frac{e^{ikx} e^{x-|x|/2}}{2\cosh\frac{x}{2}}\, dx,$$

$$\tilde{K}_2(k) = \frac{1}{2\pi} \int_{-\infty}^{+\infty} \frac{e^{ikx} e^{-x-|x|/2}}{2\cosh\frac{x}{2}}\, dx.$$

Comparing the two systems of Eqs. (10) and (11) and their corresponding expressions for the free energy, we notice that (a) $\ln[1 + \tilde{\eta}_1(k)] = \ln[1 + \tilde{a}_1(k)] + \ln[1 + \tilde{a}_2(k)]$ and (b) the driving terms (modulo the magnetic field) in the QTM system are the same as the driving term of the integral equation for $\ln \tilde{\eta}_1(k)$. Due to the similar form of the TBA equations for the XXX spin chain (10), with practically general function $\tilde{f}$, and the 2CBG (5) it is natural that a similar system like (11) can be derived via (a) $k \to k/c$, (b) $\ln[1 + \eta_1(k)] = \ln[1 + a_1(k)] + \ln[1 + a_2(k)]$, and (c) replacement of the driving terms with $-\beta(k^2 - \mu \mp H) + a_3 * f * \ln[1 + \eta_1(k)] = -\beta(k^2 - \mu \mp H) + a_3 * f * \{\ln[1 + a_1(k)] + \ln[1 + a_2(k)]\}$. Performing these transformations we obtain (6) for the grand-canonical potential and the following system of integral equations:

$$\ln a_1(k) = -\beta(k^2 - \mu + H) + (a_3 * f + \tilde{K}_0) * \ln[1 + \tilde{a}_1(k)] + (a_3 * f - \tilde{K}_2) * \ln[1 + \tilde{a}_2(k)], \tag{12a}$$

$$\ln a_2(k) = -\beta(k^2 - \mu - H) + (a_3 * f - \tilde{K}_1) * \ln[1 + \tilde{a}_1(k)] + (a_3 * f + \tilde{K}_0) * \ln[1 + \tilde{a}_2(k)]. \tag{12b}$$

Finally, it is easy to show that $(a_3 * f + \tilde{K}_0)(k) = K_0^B(k)$, $(a_3 * f - \tilde{K}_2)(k) = K_1^B(k + i\epsilon)$, $(a_3 * f - \tilde{K}_1)(k) = K_2^B(k - i\epsilon)$ by taking the Fourier transform and applying the convolution theorem, completing the derivation.

III. DENSITY PROFILES AND LOCAL CORRELATION FUNCTIONS

The experimentally relevant case of a trapped system $[V(x) \neq 0$ in (1)$]$ can be investigated using the exact solution of the uniform system [Eqs. (6) and (7)] and the local density approximation. Under this approximation, which is valid for a slowly varying potential, the system in a trap can be described locally [73] as a uniform gas with chemical potential and magnetic field defined by

$$\mu(x) = \mu(0) - V(x), \quad H(x) = H(0), \tag{13}$$

with $\mu(0)$ and $H(0)$ the chemical potential and magnetic field in the center of the trap. Therefore, for given values of temperature T, coupling strength c, chemical potential and magnetic field in the center of the trap $\mu(0)$ and $H(0)$, relevant thermodynamic quantities at a distance x from the center of the trap can be computed using Eqs. (6) and (7) with μ and H replaced by (13).

In this section, we will be mainly concerned with the calculation of the density profiles in the trap and the normalized finite-temperature local density-density correlator $g_2^{(T)}$ [73,80,81]. For a uniform system in thermal equilibrium, the linear densities of the two types of bosons can be obtained

from the derivatives of the grand-canonical potential per unit length (6):

$$n_1 = -\frac{1}{2}\left(\frac{\partial\phi}{\partial\mu} + \frac{\partial\phi}{\partial H}\right), \quad n_2 = -\frac{1}{2}\left(\frac{\partial\phi}{\partial\mu} - \frac{\partial\phi}{\partial H}\right). \quad (14)$$

In the case of the local correlator, as it was shown in [73], a simple application of the Hellmann-Feynman theorem allows to express this important observable as the derivative of the grand-canonical potential with respect to the coupling strength

$$g_2^{(T)}(x) = \frac{\sum_{a,b}\langle\Psi_a^\dagger(x)\Psi_b^\dagger(x)\Psi_a(x)\Psi_b(x)\rangle_T}{\left[\sum_a\langle\Psi_a^\dagger(x)\Psi_a(x)\rangle_T\right]^2} = \frac{1}{\left(\sum_a n_a\right)^2}\frac{\partial\phi}{\partial c}. \quad (15)$$

The local density correlation function of the uniform system which presents a nonmonotonic behavior as a function of temperature was investigated by Caux, Klauser, and van den Brink in [56,57].

A uniform 2CBG can be described with the help of three dimensionless parameters: interaction parameter $\gamma \equiv c/(n_1+n_2) = c/n$, reduced temperature $\tau \equiv T/T_d = T/n^2$, and polarization $P \equiv (n_1-n_2)/(n_1+n_2)$. While this description can be naturally extended to the inhomogeneous case by replacing the density n with the local value in the trap $n(x)$, it is preferable to work (see Ref. [73]) with

$$\gamma(x) = \frac{c}{n(x)}, \quad t = \frac{T}{c^2}, \quad P(x) = \frac{n_1(x)-n_2(x)}{n_1(x)+n_2(x)}, \quad (16)$$

where we have introduced a temperature parameter $t = \tau(x)/\gamma^2(x)$ which has the advantage of not depending on the local density $n(z)$ and characterizes the entire system in thermal equilibrium.

A. Regimes in a trapped and uniform 2CBG

Analytical results on the local density correlation function of the 2CBG at arbitrary polarization (any value of H) are very scarce in the literature (a notable exception is [57]). However, in the case when the system is fully polarized ($P = 1$), the 2CBG is equivalent to the Lieb-Liniger model for which a classification of different regimes exist. The fully polarized case represents a good starting point for the investigation of the $\gamma - t - P$ parameter space if we take into account that 1D bosons favor ferromagnetic behavior for spin-independent interactions.

In the case of the Lieb-Liniger gas, Kheruntsyan, Gangardt, Drummond, and Shlyapnikov [73,81] identified three regimes (each containing two subregimes) using the properties of the local density correlator as a function of coupling strength and temperature. Using γ and t as parameters these regimes can be characterized as follows:

Strong coupling regime. In the limit of strong interaction (or low densities) $\gamma \gg 1$, the system becomes equivalent with a system of free fermions and therefore the local density correlation function is suppressed $g_2^{(T)} \ll 1$, as a consequence of the fermionic nature of the wave functions. Two subregimes are distinguished: (a) Tonks-Girardeau (TG) characterized by $\gamma \gg 1$ and temperature smaller than the degeneracy temperature $t \ll \gamma^{-2}$ and (b) high-temperature Tonks-Girardeau for which $\gamma^{-2} \ll t \ll 1$.

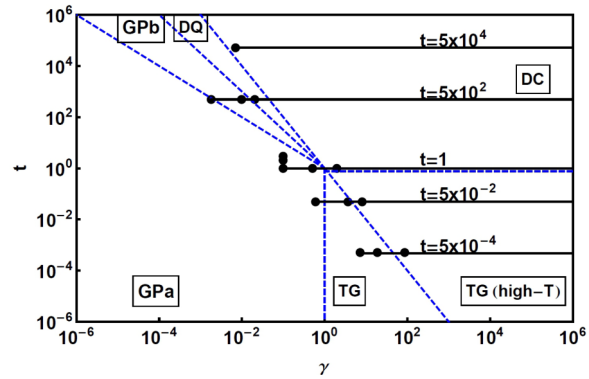

FIG. 2. (Color online) Diagram of the different regimes of the fully polarized uniform 2CBG (Lieb-Liniger model) in the γ-t plane (boundaries depicted as dashed lines) [73]. The six regimes depicted are defined as follows: Tonks-Girardeau (TG) $\gamma \gg 1$, $t \ll \gamma^{-2}$; high-temperature Tonks-Girardeau (TG-high T) $\gamma \gg 1$, $\gamma^{-2} \ll t \ll 1$; Gross-Pitaevskii a (GPa) $\gamma \ll 1$, $t \ll \gamma^{-1}$; Gross-Pitaevskii b (GPb) $\gamma^{-1} \ll t \ll \gamma^{-3/2}$; decoherent quantum (DQ) $\gamma^{-3/2} \ll t \ll \gamma^{-2}$; decoherent classical $t \gg \max(\gamma^{-2},1)$. The black dots are the values of $\gamma(0)$ and t in the center of the trap of the representative systems considered in the next section with the continuous black lines at $t = \{5\times10^{-4}, 5\times10^{-2}, 1, 5\times10^{2}, 5\times10^{4}\}$ representing the values of $\gamma(x)$ in the trap for these systems.

Gross-Pitaevskii regime. In the limit of vanishing interactions (or large densities) $\gamma \ll 1$, the local density correlation function approaches $g_2^{(T)} \simeq 1$ which is the value for free bosons. The two subregimes are Gross-Pitaevskii a ($\gamma \ll 1$, $t \ll \gamma^{-1}$) and Gross-Pitaevskii b ($\gamma^{-1} \ll t \ll \gamma^{-3/2}$).

Decoherent regime. At high temperatures, the local pair correlation is close to $g_2^{(T)} \simeq 2$. The two subregimes are decoherent quantum (DQ) ($\gamma^{-3/2} \ll t \ll \gamma^{-2}$) and decoherent classical (DC) [$t \gg \max(\gamma^{-2},1)$].

For a trapped system, this classification still remains valid with the possibility of different regimes coexisting within the trap. Due to the fact that for large distances from the center of the trap the density vanishes $n(x) \to 0, \gamma(x) \to \infty$ this means that the tails of the system are always in the TG regime (for $t < 1$) or the DC regime (for $t > 1$). For given values of the interaction and temperature parameters $\gamma(0)$ and t, the density profile follows a straight line at t parallel with the γ axis as it is shown in Fig. 2 for $t = \{5\times10^{-4}, 5\times10^{-2}, 1, 5\times10^{2}, 5\times10^{4}\}$. All these considerations are valid for the fully polarized 2CBG. In the following sections, we are going to investigate the influence of the polarization on the density profiles and local density correlation function.

B. Density profiles and local correlation functions at high temperatures

For a given value of the coupling strength c, the region of high temperatures is defined by $t \gg 1$. We have calculated the density profiles and the local correlation function on a fine grid of the trap using Eqs. (6), (7), (14), (15), and the LDA chemical potential and magnetic field (13). The results for three values of $\gamma(0)$ at $t = 5\times10^2$ and various polarizations are shown in Fig. 3. In Fig. 3, the distance x is plotted in units of the Thomas-Fermi radius in the Gross-Pitaevskii regime [73]

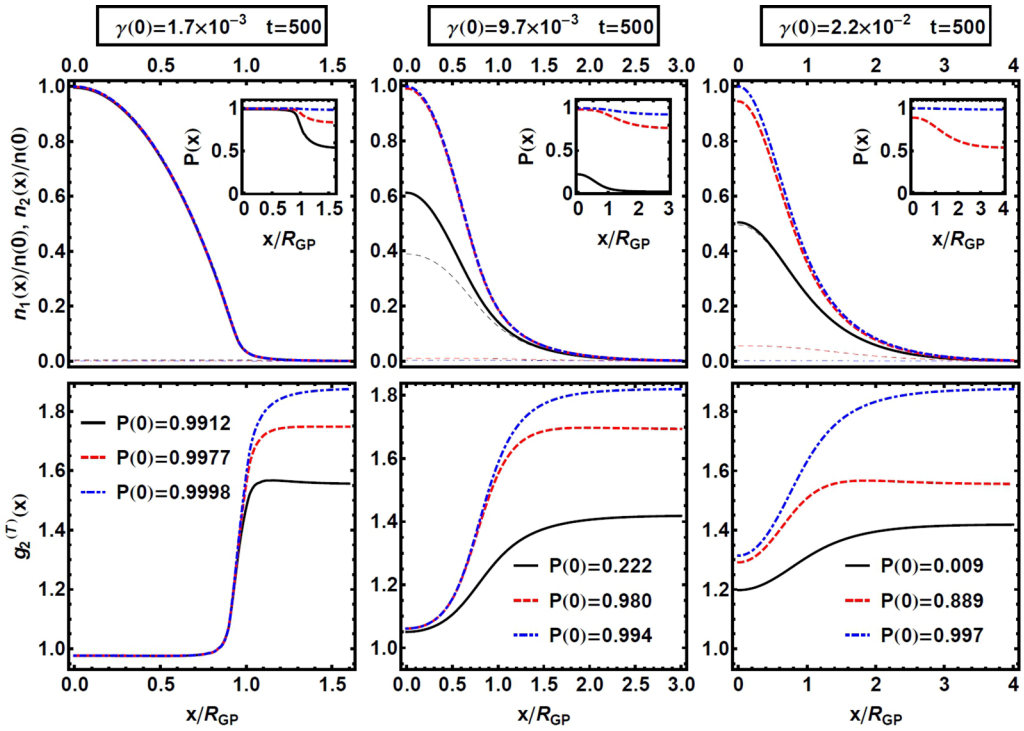

FIG. 3. (Color online) Density profiles (upper panels) and local density correlation function $g_2^{(T)}(x)$ (lower panels) of a trapped 2CBG at temperature $t = 5 \times 10^2$ for three values of $\gamma(0) = \{1.7 \times 10^{-3}, 9.7 \times 10^{-3}, 2.2 \times 10^{-2}\}$ and various polarizations. In the upper panels, the thick continuous, thick dashed, and thick dotted-dashed (thin continuous, thin dashed, and thin dotted-dashed) lines represent the majority (minority) components and $n(0)$ is the total density in the center of the trap. The insets depict the variation of the polarization in the trap.

$R_{\rm GP} = (6Nc/\omega^2)^{1/3}$ with N the number of particles in the trap $N = \int [n_1(x) + n_2(x)]\,dx$, and ω is the trap oscillation frequency. The left panels of Fig. 3 depict the situation in which the gas in the center of the trap is in the GPa regime with three polarizations very close to 1 [see Fig. 2 where $\gamma(0) = 1.7 \times 10^{-3}$ is the leftmost point on the $t = 5 \times 10^2$ line] for which $g_2^{(T)}(0) \simeq 1$. While in the center of the trap the local correlator is almost constant showing no dependence on $P(0)$, the situation changes dramatically in the tails where the gas is in the DC regime. Here, we see that even small variations of the center polarization have a significant effect in the tail behavior of the local correlator and polarization. For larger values of $\gamma(0)$ (center and right panels of Fig. 3), the effect of the polarization in the center of the trap on the local correlation function becomes more pronounced with $g_2^{(T)}(x)$ increasing both as a function of γ and $P(0)$. In addition, we see that the density profiles present larger tails as we approach the DC regime.

For large values of γ and t, when the 2CBG is in the DC regime, it can be shown using Wick's theorem and Boltzmann distribution [56,57] that for a uniform system the asymptotic values of the local correlator and polarization are

$$g_2^{(T)} = 1 + \frac{e^{2\beta(\mu+H)} + e^{2\beta(\mu-H)}}{(e^{\beta(\mu+H)} + e^{\beta(\mu-H)})^2}, \quad P = \frac{e^{\beta(\mu+H)} - e^{\beta(\mu-H)}}{e^{\beta(\mu+H)} + e^{\beta(\mu-H)}}. \tag{17}$$

This means that in the case of a trapped system at very large temperatures, the local correlator at the edge of the sample should tend asymptotically to 2 for $P(0) = 1$ (very large magnetic field) and to 1.5 for $P(0) = 0$ (vanishing magnetic field). This can be seen clearly in Fig. 4 where we present the density profiles and local correlator for $t = 5 \times 10^4$ and $\gamma(0) = 7 \times 10^{-3}$. Here, the entire sample is in the DC regime and the effect of $P(0)$ on $g_2^{(T)}$ is very large.

C. Density profiles and local correlation functions at intermediate temperatures

For temperatures close to 1 we can encounter the situation in which for small variations of t the profile of the local correlation function changes drastically as it can be seen in the left panels of Fig. 5 for the fully polarized gas with $\gamma(0) = 0.11$ and $t = \{1,2,3\}$. While the density profiles are almost identical, $g_2^{(T)}(x)$ presents a highly nonmonotonic behavior with asymptotic values at the edge of the samples varying from 0.65 for $t = 1$ to 1.05 for $t = 3$. A similar phenomenon can be seen for fixed temperature and various polarizations in the center and right panels of Fig. 5. For $t = 1$ and $\gamma(0) = 0.5$, the local correlation functions are almost equal in the center of the system but for large distances $g_2^{(T)}(x)$ is suppressed for small polarizations and enhanced for large polarizations. The role of $P(0)$ increases at strong coupling [large $\gamma(0)$] as shown in the right panel where for $\gamma(0) = 1.94$ and $t = 1$ the local correlators present a strong dependence on the polarization even in the center of the trap.

D. Density profiles and local correlation functions at low temperatures

At low temperatures ($t \ll 1$), the edges of the system will always be in the TG regime and, therefore, the local

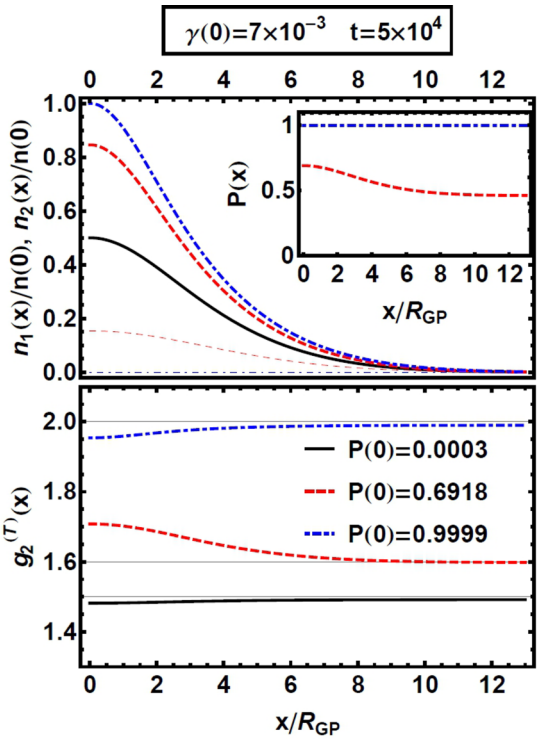

FIG. 4. (Color online) Density profiles (upper panel) and local density correlation function $g_2^{(T)}(x)$ (lower panel) of a trapped 2CBG at temperature $t = 5 \times 10^4$ for $\gamma(0) = 7 \times 10^{-3}$ and polarizations $P(0) = \{0.0003, 0.6918, 0.9999\}$. In the upper panels the thick continuous, thick dashed, and thick dotted-dashed (thin continuous, thin dashed, and thin dotted-dashed) lines represent the majority (minority) components and $n(0)$ is the total density in the center of the trap. The inset depicts the variation of the polarization in the trap. In the lower panel, the thin lines denote the asymptotic values given by Eq. (17).

correlator will be strongly suppressed. In addition, we expect the density profiles to be sharper as it can be seen in Fig. 6 for $t = 5 \times 10^{-2}$. As expected, $g_2^{(T)}(x)$ decreases in the tails of the distribution until it reaches a limiting value which depends on $\gamma(0)$. The influence of the center polarization becomes more pronounced at stronger coupling with $g_2^{(T)}(0)$ monotonically increasing as a function of $P(0)$. It should be noted that numerical investigations at low temperatures and low polarizations ($H \to 0$) are very difficult due to the fact that in this regime the NLIEs (7) become numerically unstable [the same phenomenon happens in the case of the TBA equations (5)] as a consequence of the first-order phase transition at $T = 0, H = 0$. For $t = 5 \times 10^{-4}$, results are shown in Fig. 7.

The numerical data presented above show that the polarization at the center of the trap has a profound influence on the density profiles and the local density correlation function of the inhomogeneous system. $g_2^{(T)}(0)$ is a monotonic increasing function of $P(0)$ with the influence of the center polarization being more pronounced at strong coupling. Also, the local correlation function which takes a wide range of values between 0 and 2 serves as a better discriminant than the density profiles for the different regimes of the 2CBG.

IV. 2CBG AS THE CONTINUUM LIMIT OF THE PERK-SCHULTZ SPIN CHAIN WITH (− − −) GRADING

Our method of deriving the thermodynamic description of the 2CBG [Eqs. (6) and (7)] is based on the fact that the continuum model can be obtained by performing a specific limit of an appropriate lattice model for which the quantum transfer matrix technique can be employed. For the two-component Bose gas, the relevant lattice model is the $q = 3$ Perk-Schultz spin chain. In this section, we are going to present this scaling limit and show how the grand-canonical partition function of the 2CBG can be derived from the canonical partition function of the spin chain.

The Hamiltonian of the $q = 3$ Perk-Schultz spin chain with arbitrary grading is [61–64]

$$\mathcal{H}_{PS} = J\varepsilon_1 \sum_{j=1}^{L} \left[\cos\gamma \sum_{a=1}^{3} \varepsilon_a e_{aa}^{(j)} e_{aa}^{(j+1)} + \sum_{\substack{a,b=1 \\ a\neq b}}^{3} e_{ab}^{(j)} e_{ba}^{(j+1)} + i\sin\gamma \sum_{\substack{a,b=1 \\ a\neq b}}^{3} \mathrm{sgn}(a-b) e_{aa}^{(j)} e_{bb}^{(j+1)} \right] - \sum_{j=1}^{L}\sum_{a=1}^{3} h_a e_{aa}^{(j)}, \tag{18}$$

where L is the number of lattice sites, $\gamma \in (0,\pi)$ determines the anisotropy ($q = e^{i\gamma}$), $J > 0$ determines the strength of the interaction, and h_a are chemical potentials. The parameters $(\varepsilon_1,\varepsilon_2,\varepsilon_3)$ can take the values ± 1 and we will call them the grading of the system. In (18), $e_{ab}^{(j)} = \mathbb{I}_3^{\otimes j-1} \otimes e_{ab} \otimes \mathbb{I}_3^{\otimes L-j}$, with e_{ab} the 3×3 matrix with elements $(e_{ab})_{ij} = \delta_{ai}\delta_{bj}$ and $\mathbb{I}_3$ the 3×3 unit matrix. The Perk-Schultz Hamiltonian is the sum of $\mathcal{H}_b$ (in the brackets) which is the fundamental spin-model associated with the trigonometrical Perk-Schultz R matrix [62] and $\mathcal{H}_c$ the chemical potential part which does not break the integrability. In the next section and Appendix A, we will show that for $(\varepsilon_1,\varepsilon_2,\varepsilon_3) = (- - -)$ the energy spectrum is

$$E_{\mathrm{PS}} = \sum_{j=1}^{M} e_0\left(v_j^{(1)}\right) + M_1(h_2 - h_3) + E_0,$$
$$e_0(v) = J\frac{\sin^2\gamma}{\sin(v-\gamma)\sin v} + h_1 - h_2, \quad E_0 = JL\cos\gamma - h_1 L, \tag{19}$$

with $\{v_j^{(1)}\}_{j=1}^{M}$ satisfying the BAEs

$$\left[\frac{\sin\left(\gamma - v_s^{(1)}\right)}{\sin v_s^{(1)}}\right]^L = \prod_{\substack{j=1 \\ j\neq s}}^{M} \frac{\sin\left(v_s^{(1)} - v_j^{(1)} - \gamma\right)}{\sin\left(v_s^{(1)} - v_j^{(1)} + \gamma\right)} \times \prod_{p=1}^{M_1} (-) \frac{\sin\left(v_s^{(1)} - v_p^{(2)} + \gamma\right)}{\sin\left(v_s^{(1)} - v_p^{(2)}\right)}, \quad s = 1,\ldots,M \tag{20a}$$

$$\prod_{j=1}^{M} (-) \frac{\sin\left(v_l^{(2)} - v_j^{(1)} - \gamma\right)}{\sin\left(v_l^{(2)} - v_j^{(1)}\right)} = \prod_{\substack{p=1 \\ p\neq l}}^{M_1} \frac{\sin\left(v_l^{(2)} - v_p^{(2)} - \gamma\right)}{\sin\left(v_l^{(2)} - v_p^{(2)} + \gamma\right)}, \quad l = 1,\ldots,M_1. \tag{20b}$$

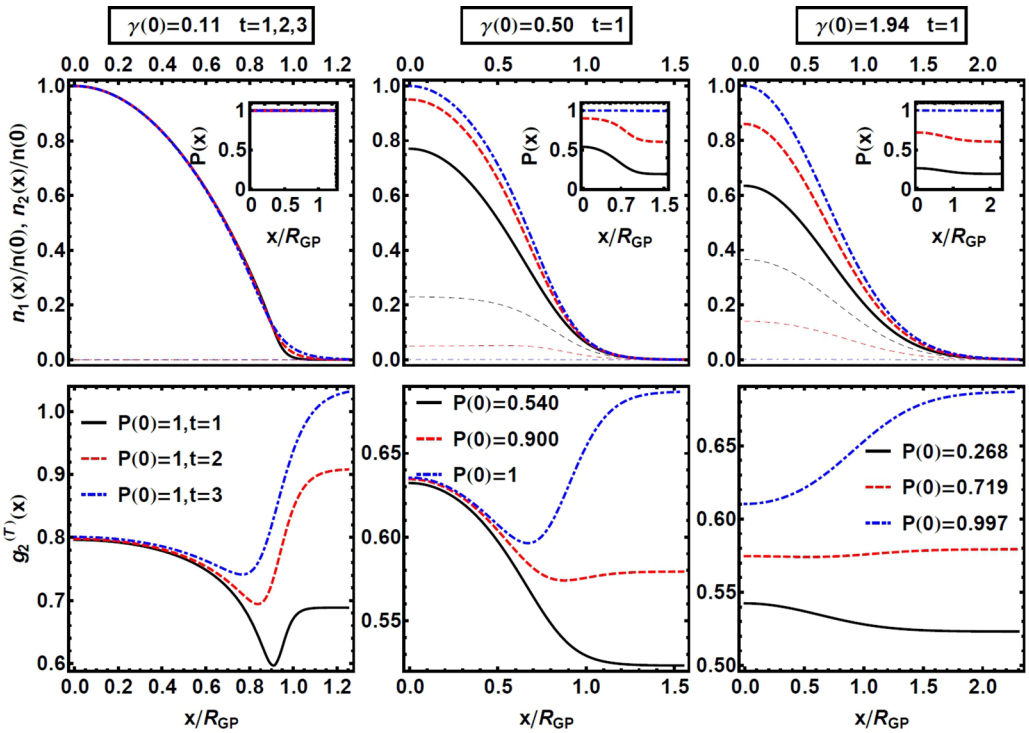

FIG. 5. (Color online) Density profiles (upper panels) and local density correlation function $g_2^{(T)}(x)$ (lower panels) of a trapped 2CBG at different temperatures and polarizations for three values of $\gamma(0) = \{0.11,0.5,1.94\}$ and various polarizations. In the upper panels, the thick continuous, thick dashed, and thick dotted-dashed (thin continuous, thin dashed, and thin dotted-dashed) lines represent the majority (minority) components and $n(0)$ is the total density in the center of the trap. The insets depict the variation of the polarization in the trap.

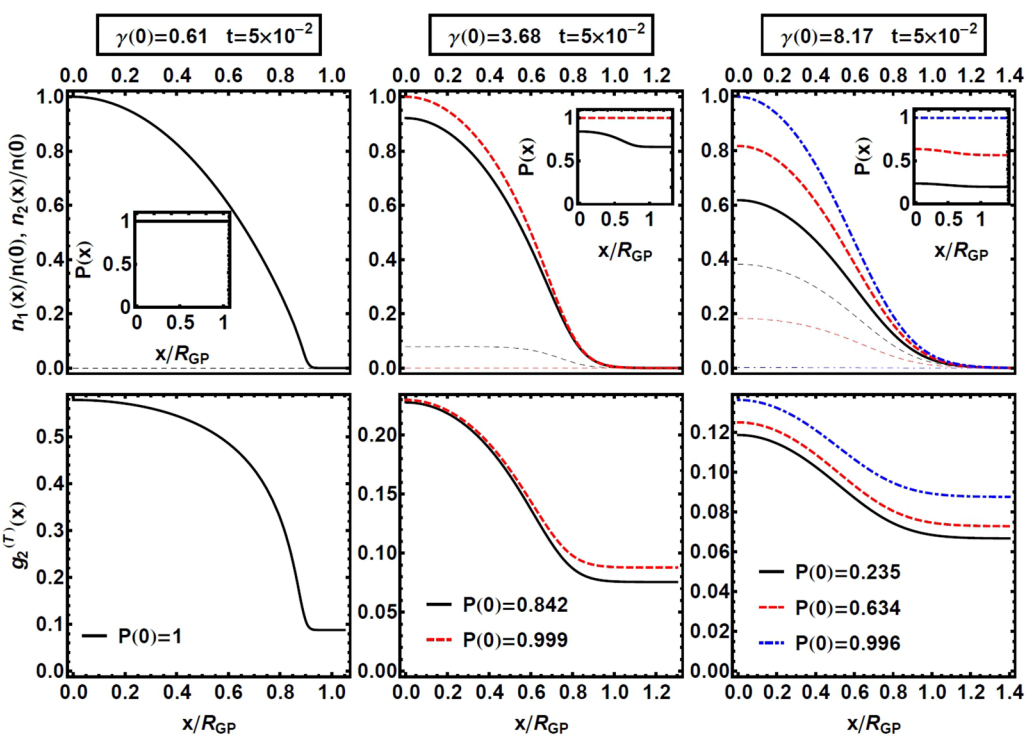

FIG. 6. (Color online) Density profiles (upper panels) and local density correlation function $g_2^{(T)}(x)$ (lower panels) of a trapped 2CBG at temperature $t = 5 \times 10^{-2}$ for three values of $\gamma(0) = \{0.61,3.68,8.17\}$ and various polarizations. In the upper panels the thick continuous, thick dashed, and thick dotted-dashed (thin continuous, thin dashed, and thin dotted-dashed) lines represent the majority (minority) components and $n(0)$ is the total density in the center of the trap. The insets depict the variation of the polarization in the trap.

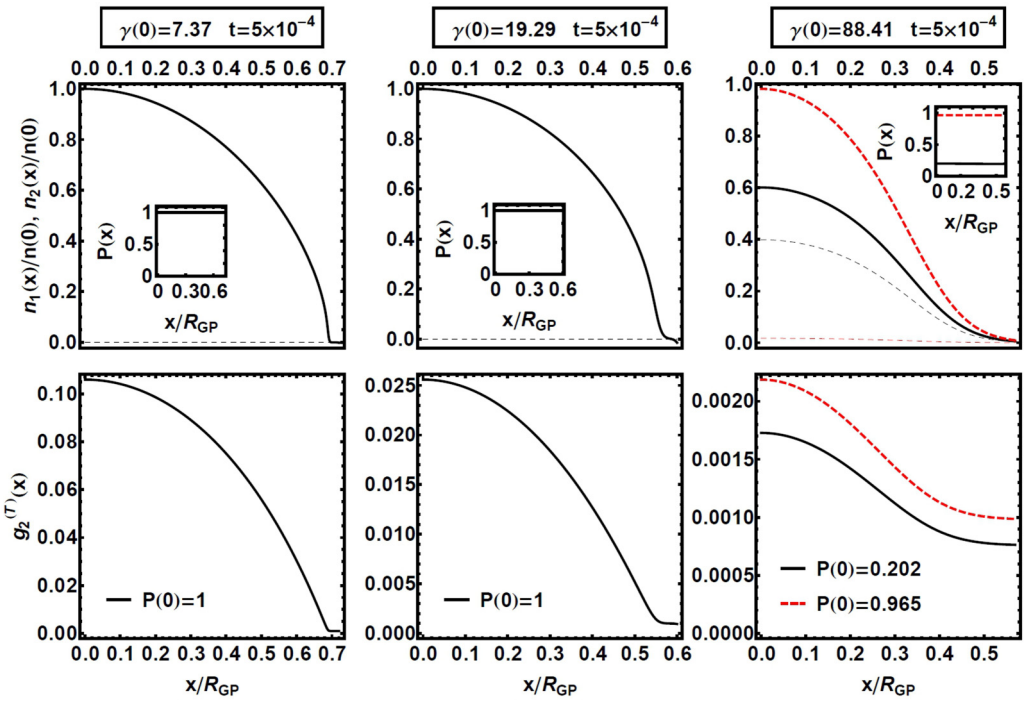

FIG. 7. (Color online) Density profiles (upper panels) and local density correlation function $g_2^{(T)}(x)$ (lower panels) of a trapped 2CBG at temperature $t = 5 \times 10^{-4}$ for three values of $\gamma(0) = \{7.37, 19.29, 88.41\}$ and various polarizations. In the upper panels, the thick continuous, thick dashed (thin continuous, thin dashed) lines represent the majority (minority) components and $n(0)$ is the total density in the center of the trap. The insets depict the variation of the polarization in the trap.

First, we will show how the BAEs (3) of the 2CBG can be obtained from the BAEs (20) of the Perk-Schultz spin chain. The spin chain is characterized by the following set of parameters: number of lattice sites L, anisotropy γ, strength of the interaction $J > 0$, lattice constant δ, and chemical potentials h_1, h_2, h_3. Consider $v_s^{(1)} \to i\delta k_s^{(1)}/\epsilon + \gamma/2$ and $v_s^{(2)} \to i\delta k_s^{(2)}/\epsilon + \gamma + \pi/2$ with $\epsilon \to 0$. The BAEs (20) become

$$\left[(-)\frac{\sinh\left(\delta k_s^{(1)}/\epsilon - i\gamma/2\right)}{\sinh\left(\delta k_s^{(1)}/\epsilon + i\gamma/2\right)}\right]^L = \prod_{\substack{j=1\\ j\neq s}}^{M} \frac{\sinh\left(\delta k_s^{(1)}/\epsilon - \delta k_j^{(1)}/\epsilon - i\gamma\right)}{\sinh\left(\delta k_s^{(1)}/\epsilon - \delta k_j^{(1)}/\epsilon + i\gamma\right)} \prod_{p=1}^{M_1}(-)\frac{\cosh\left(\delta k_s^{(1)}/\epsilon - \delta k_p^{(2)}/\epsilon + i\gamma/2\right)}{\cosh\left(\delta k_s^{(1)}/\epsilon - \delta k_p^{(2)}/\epsilon - i\gamma/2\right)},$$

$$\prod_{j=1}^{M}(-)\frac{\cosh\left(\delta k_l^{(2)}/\epsilon - \delta k_j^{(1)}/\epsilon + i\gamma/2\right)}{\cosh\left(\delta k_l^{(2)}/\epsilon - \delta k_j^{(1)}/\epsilon - i\gamma/2\right)} = \prod_{\substack{p=1\\ p\neq l}}^{M_1} \frac{\sinh\left(\delta k_l^{(2)}/\epsilon - \delta k_p^{(2)}/\epsilon + i\gamma\right)}{\sinh\left(\delta k_l^{(2)}/\epsilon - \delta k_p^{(2)}/\epsilon - i\gamma\right)}.$$

In the second step we perform $\gamma = \pi - \epsilon$ with the result

$$\left[\frac{\cosh\left(\delta k_s^{(1)}/\epsilon + i\epsilon/2\right)}{\cosh\left(\delta k_s^{(1)}/\epsilon - i\epsilon/2\right)}\right]^L = \prod_{\substack{j=1\\ j\neq s}}^{M} \frac{\sinh\left(\delta k_s^{(1)}/\epsilon - \delta k_j^{(1)}/\epsilon + i\epsilon\right)}{\sinh\left(\delta k_s^{(1)}/\epsilon - \delta k_j^{(1)}/\epsilon - i\epsilon\right)} \prod_{p=1}^{M_1} \frac{\sinh\left(\delta k_s^{(1)}/\epsilon - \delta k_p^{(2)}/\epsilon - i\epsilon/2\right)}{\sinh\left(\delta k_s^{(1)}/\epsilon - \delta k_p^{(2)}/\epsilon + i\epsilon/2\right)}, \tag{21a}$$

$$\prod_{j=1}^{M} \frac{\sinh\left(\delta k_l^{(2)}/\epsilon - \delta k_j^{(1)}/\epsilon - i\epsilon/2\right)}{\sinh\left(\delta k_l^{(2)}/\epsilon - \delta k_j^{(1)}/\epsilon + i\epsilon/2\right)} = \prod_{\substack{p=1\\ p\neq l}}^{M_1} \frac{\sinh\left(\delta k_l^{(2)}/\epsilon - \delta k_p^{(2)}/\epsilon - i\epsilon\right)}{\sinh\left(\delta k_l^{(2)}/\epsilon - \delta k_p^{(2)}/\epsilon + i\epsilon\right)}. \tag{21b}$$

Finally, taking the limit $L \to \infty$ like $O(1/\epsilon^2)$, $\delta \to 0$ like $O(\epsilon^2)$, such that $L_B = L\delta$ and $c = \epsilon^2/\delta$, equating $M_1 = M_1^B$ and using

$$\frac{\cosh\left(\delta k_s^{(1)}/\epsilon + i\epsilon/2\right)}{\cosh\left(\delta k_s^{(1)}/\epsilon - i\epsilon/2\right)} \sim \frac{1 + ik_s^{(1)}\delta/2}{1 - ik_s^{(1)}\delta/2},$$

TABLE I. Parameters for the $(---)$ Perk-Schultz spin chain and the spinor Bose gas.

$(---)$ Perk-Schultz spin chain	Spinor Bose gas
Lattice constant $\delta \to O(\epsilon^2)$	Particle mass $m = \frac{1}{2}$
Number of lattice sites $L \to O(1/\epsilon^2)$	Physical length $L_B = L\delta$
Interaction strength $J > 0$	Repulsion strength $c = \epsilon^2/\delta$
Chemical potential $h_1 \to O(\epsilon^2)$	Chemical potential $\mu = \frac{J\epsilon^2}{\delta^2} - \frac{h_1}{\delta^2} + \frac{J\epsilon^4}{4\delta^2} + \frac{1}{2\delta^2}(h_3 + h_2)$
Chemical potentials $h_2, h_3 \to O(\epsilon^4)$	Magnetic field $H = (h_3 - h_2)/(2\delta^2)$
Inverse temperature β	Inverse temperature $\overline{\beta} = \beta\delta^2$
Anisotropy $\gamma = \pi - \epsilon$	

we find that (21) transform into the BAEs (3) of the Bose gas. Performing the same transformations in the expression for the energy we obtain

$$E_{\rm PS} - E_0 = \sum_{j=1}^{M} \left[J\delta^2 \left(k_j^{(1)}\right)^2 - J\epsilon^2 - J\epsilon^4/4 \right] + (h_1 - h_2)M + (h_2 - h_3)M_1 + O(\epsilon^6), \quad (22)$$

which shows that in order to obtain the energy spectrum of the Bose gas (2) we need to scale $J \to \infty$ like $O(1/\epsilon^4)$ and $h_1 \to \infty$ like $O(1/\epsilon^2)$ such that $J\delta^2 = 1$ and $J\epsilon^2 + J\epsilon^4/4 - h_1 + h_2$ is finite. Therefore, in the thermodynamic limit performing this scaling we have

$$e^{\beta E_0} Z(h_1,h_2,h_3,\beta) \to \mathcal{Z}(\mu,H,\beta), \quad (23)$$

where $\beta = 1/T$, $Z(h_1,h_2,h_3,\beta)$ is the canonical partition function of the spin chain, and $\mathcal{Z}(\mu,H,\beta)$ is the grand-canonical partition function of the 2CBG.

This scaling limit is independent of the temperature of the systems. However, taking into account that we are interested in the thermodynamic behavior it is more useful to introduce a scaling limit which involves also the temperature. This is justified because from the thermodynamics point of view, the energy spectrum enters via the expression $e^{-\beta E}$. Multiplying with β the identity (22) we find that $\beta(E_{\rm PS} - E_0) = \bar{\beta} E_{\rm Bose}$, with $\bar{\beta}$ the inverse temperature in the continuum system, if $\beta = \bar{\beta}/\delta^2$, $J = 1$ $h_1 \to 0$ like $O(\epsilon^2)$, such that $J\epsilon^2/\delta^2 - h_1/\delta^2$ is finite and $h_2, h_3 \to 0$ like $O(\epsilon^4)$. In this case, Eq. (23) becomes

$$e^{\beta E_0} Z(h_1,h_2,h_3,\beta) \to \mathcal{Z}(\mu,H,\bar{\beta}). \quad (24)$$

In Table I we present in a compact form this continuum limit (the spectral parameter in the lattice model scales like $v \to i\delta k/\epsilon$) which will be used in the next sections to derive the thermodynamic behavior of the 2CBG from similar result for the $(---)$ Perk-Schultz spin chain.

V. ALGEBRAIC BETHE ANSATZ AND THE QUANTUM TRANSFER MATRIX OF THE $(---)$ PERK-SCHULTZ SPIN CHAIN

In the next section, we are going to derive a finite set of NLIEs characterizing the thermodynamics of the $(---)$ Perk-Schultz spin chain using the associated quantum transfer matrix. Therefore, it will be useful to recall some basic notions of algebraic Bethe ansatz [82].

A. ABA for the Hamiltonian

The Hamiltonian (18) represents the fundamental spin model (Chap. VI of [82]) associated with the trigonometric $q = 3$ Perk-Schultz R matrix [62,63] defined by

$$\mathsf{R}(v,w) = \sum_{a=1}^{3} \mathsf{R}_{aa}^{aa}(v,w) e_{aa} \otimes e_{aa} + \sum_{\substack{a,b=1\\ a\neq b}}^{3} \mathsf{R}_{ab}^{ab}(v,w)\, e_{aa} \otimes e_{bb} + \sum_{\substack{a,b=1\\ a\neq b}}^{3} \mathsf{R}_{ba}^{ab}(v,w)\, e_{ab} \otimes e_{ba}, \quad (25)$$

with[2]

$$\mathsf{R}_{aa}^{aa}(v,w) = \frac{\sin[\gamma + \varepsilon_a(v-w)]}{\sin\gamma}, \qquad \mathsf{R}_{ab}^{ab}(v,w) \underset{a\neq b}{=} \frac{\sin(v-w)}{\sin\gamma}, \qquad \mathsf{R}_{ba}^{ab}(v,w) \underset{a\neq b}{=} e^{i\,sgn(a-b)(v-w)}, \quad (26)$$

and $(e_{ab})_{ij} = \delta_{ia}\delta_{jb}$ the canonical basis in the space of 3×3 matrices. This 9×9 R matrix has the property that $\mathsf{R}(0,0) = \mathsf{P}$, with $\mathsf{P}_{b_1 b_2}^{a_1 a_2} = \delta_{a_1 b_2}\delta_{a_2 b_1}$ the permutation matrix, and satisfies the Yang-Baxter equation

$$\sum_{a',b',c'=1}^{3} \mathsf{R}_{a'b'}^{a\ b}(v,w)\mathsf{R}_{a''c'}^{a'\ c}(v,\nu)\mathsf{R}_{b''c''}^{b'\ c'}(w,\nu) = \sum_{a',b',c'=1}^{3} \mathsf{R}_{b'c'}^{b\ c}(w,\nu)\mathsf{R}_{a'c''}^{a\ c'}(v,\nu)\mathsf{R}_{a''b''}^{a'\ b'}(v,w). \quad (27)$$

Let us sketch how we can obtain the Hamiltonian (18) (more precisely, the component within the brackets) in the framework of algebraic Bethe ansatz (ABA). First, we need to introduce

[2]In [62,63] the authors considered the more general case $\mathsf{R}_{ab}^{ab}(v,w) = G_{ab}\frac{\sin(v-w)}{\sin\gamma}$ with $G_{ab}G_{ba}^{-1} = 1$ (no summation). The situation considered in our paper corresponds to $G_{ab} = 1$.

the L operators defined by

$$\mathsf{L}_j(v,0) = \sum_{a,b,a_1,b_1=1}^{3} \mathsf{R}^{aa_1}_{b\,b_1}(v,0) e^{(0)}_{ab} e^{(j)}_{a_1 b_1}, \quad \mathsf{L}_j(v,0) \in \mathrm{End}[(\mathbb{C}^3)^{\otimes(L+1)}], \tag{28}$$

where $e^{(j)}_{ab}$ is the canonical basis of operators acting on $(\mathbb{C}^3)^{\otimes(L+1)}$, i.e., $e^{(0)}_{ab} = e_{ab} \otimes \mathbb{I}_3^{\otimes L}$ and $e^{(j)}_{ab} = \mathbb{I}_3 \otimes \mathbb{I}_3^{\otimes(j-1)} \otimes e_{ab} \otimes \mathbb{I}_3^{\otimes(L-j)}$ for $j = 1,\ldots,L$. These operators act on the tensorial product of $\mathbb{C}^3$, which is called the auxiliary space, and the Hilbert space of the spin chain $\mathfrak{H} = (\mathbb{C}^3)^{\otimes L}$. In this auxiliary space, using the definition of the R matrix (25), the L operators can be represented as

$$\mathsf{L}_j(v,0) = \begin{pmatrix} \alpha_1(v,0)e^{(j)}_{11} + \beta(v,0)\big[e^{(j)}_{22} + e^{(j)}_{33}\big] & \gamma_-(v,0)e^{(j)}_{21} & \gamma_-(v,0)e^{(j)}_{31} \\ \gamma_+(v,0)e^{(j)}_{12} & \alpha_2(v,0)e^{(j)}_{22} + \beta(v,0)\big[e^{(j)}_{11} + e^{(j)}_{33}\big] & \gamma_-(v,0)e^{(j)}_{32} \\ \gamma_+(v,0)e^{(j)}_{13} & \gamma_+(v,0)e^{(j)}_{23} & \alpha_3(v,0)e^{(j)}_{33} + \beta(v,0)\big[e^{(j)}_{11} + e^{(j)}_{22}\big] \end{pmatrix}, \tag{29}$$

where we have introduced

$$\alpha_i(v,w) = \frac{\sin[\gamma + \varepsilon_i(v-w)]}{\sin\gamma}, \quad \beta(v,w) = \frac{\sin(v-w)}{\sin\gamma}, \quad \gamma_\pm(v,w) = e^{\pm i sgn(a-b)(v-w)}. \tag{30}$$

In (29), $e^{(j)}_{ab}$ now represents the canonical basis of operators acting on $(\mathbb{C}^3)^{\otimes L}$ and, therefore, the elements of the matrix represent operators acting on the Hilbert space of the spin chain. The monodromy matrix is the ordered product of L operators

$$\mathsf{T}(v) = \mathsf{L}_L(v,0)\mathsf{L}_{L-1}(v,0)\ldots\mathsf{L}_1(v,0), \quad T(v) = \begin{pmatrix} T_{11}(v) & T_{12}(v) & T_{13}(v) \\ T_{21}(v) & T_{22}(v) & T_{23}(v) \\ T_{31}(v) & T_{32}(v) & T_{33}(v) \end{pmatrix}, \tag{31}$$

and provides a representation of the Yang-Baxter algebra

$$\check{\mathsf{R}}(v,w)[\mathsf{T}(v) \otimes \mathsf{T}(w)] = [\mathsf{T}(v) \otimes \mathsf{T}(w)]\check{\mathsf{R}}(v,w), \tag{32}$$

where $\check{\mathsf{R}}^{a_1 a_2}_{b_1\,b_2}(v,w) = (\mathsf{PR})^{a_1 a_2}_{b_1\,b_2}(v,w) = \mathsf{R}^{a_2 a_1}_{b_1 b_2}(v,w)$. In Eq. (32), the tensor product should be understood as the tensor product of 3×3 matrices with operator-valued entries as presented in the right-hand side of (31). Finally, the transfer matrix is defined as the trace of the monodromy matrix in the auxiliary space

$$\mathsf{t}(v) = \mathrm{tr}_0 \mathsf{T}(v) = T_{11}(v) + T_{22}(v) + T_{33}(v). \tag{33}$$

Following [83] we can show that

$$\mathcal{H}_{\mathrm{PS}} = J\varepsilon_1 \sin\gamma\, \mathsf{t}^{-1}(0)\mathsf{t}'(0) - \sum_{j=1}^{L}\sum_{a=1}^{3} h_a e^{(j)}_{aa}. \tag{34}$$

Obtaining the eigenvalues of the transfer matrix requires the existence of a pseudovacuum on which the monodromy matrix acts triangularly. Using (29), it is easy to see that

$$|\Omega\rangle = \underbrace{\begin{pmatrix}1\\0\\0\end{pmatrix} \otimes \cdots \otimes \begin{pmatrix}1\\0\\0\end{pmatrix}}_{L \text{ times}} \tag{35}$$

satisfies the requirements of a pseudovacuum, and

$$\mathsf{T}(v)|\Omega\rangle = \begin{pmatrix} T_{11}(v)|\Omega\rangle & T_{12}(v)|\Omega\rangle & T_{13}(v)|\Omega\rangle \\ T_{21}(v)|\Omega\rangle & T_{22}(v)|\Omega\rangle & T_{23}(v)|\Omega\rangle \\ T_{31}(v)|\Omega\rangle & T_{32}(v)|\Omega\rangle & T_{33}(v)|\Omega\rangle \end{pmatrix} = \begin{pmatrix} (\alpha_1(v,0))^L|\Omega\rangle & T_{12}(v)|\Omega\rangle & T_{13}(v)|\Omega\rangle \\ 0 & (\beta(v,0))^L|\Omega\rangle & 0 \\ 0 & 0 & (\beta(v,0))^L|\Omega\rangle \end{pmatrix}. \tag{36}$$

The energy spectrum of the Perk-Schultz spin chain (19) with the $(---)$ grading is obtained using Eq. (34) and the eigenvalues of the transfer matrix (see Appendix A):

$$\begin{aligned} \tau(v) = {} & \left[\frac{\sin(\gamma - v)}{\sin\gamma}\right]^L \prod_{j=1}^{M} \frac{\sin\left(\gamma - v_j^{(1)} + v\right)}{\sin\left(v_j^{(1)} - v\right)} + \left(\frac{\sin v}{\sin\gamma}\right)^L \prod_{j=1}^{M} \frac{\sin\left(\gamma - v + v_j^{(1)}\right)}{\sin\left(v - v_j^{(1)}\right)} \prod_{i=1}^{M_1} \frac{\sin\left(\gamma - v_i^{(2)} + v\right)}{\sin\left(v_i^{(2)} - v\right)} \\ & + \left(\frac{\sin v}{\sin\gamma}\right)^L \prod_{j=1}^{M_1} \frac{\sin\left(\gamma - v + v_j^{(2)}\right)}{\sin\left(v - v_j^{(2)}\right)}, \end{aligned} \tag{37}$$

with $\{v_j^{(1)}\}_{j=1}^{M}, \{v_i^{(2)}\}_{j=1}^{M_1}$ satisfying the BAEs (20), and the fact that the contribution of the chemical potential component is given by $M(h_1 - h_2) + M_1(h_2 - h_3) + E_0$ [62].

B. ABA for the quantum transfer matrix

The quantum transfer matrix [65,68] is an algebraic object which plays a significant role in the investigation of finite-temperature properties of integrable systems. The importance of the QTM resides in the fact that not only the free energy can be derived from the largest eigenvalue, but also that different correlation lengths can be characterized as ratios of the leading eigenvalues. Pedagogical introductions in the subject can be found in [84–86].

In order to introduce the QTM we need to define two types of L operators $\mathsf{L}_j(v,-u)$, $\tilde{\mathsf{L}}_j(u,v) \in \mathrm{End}[(\mathbb{C}^3)^{\otimes(N+1)}]$ as

$$\mathsf{L}_j(v,-u) = \sum_{a,b,a_1,b_1=1}^{3} \mathsf{R}_{b\,b_1}^{a\,a_1}(v,-u) e_{ab}^{(0)} e_{a_1 b_1}^{(j)}, \quad \tilde{\mathsf{L}}_j(u,v) = \sum_{a,b,a_1,b_1=1}^{3} \mathsf{R}_{a_1\,b}^{b_1\,a}(u,v) e_{ab}^{(0)} e_{a_1 b_1}^{(j)}, \tag{38}$$

where $u = -J\sin(\varepsilon_1\gamma)\frac{\beta}{N}$, with $N \in 4\mathbb{N}$ the Trotter number, and $e_{ab}^{(j)}$ is a canonical basis of operators acting on $(\mathbb{C}^3)^{\otimes(N+1)}$. In the auxiliary space, the L operators can be represented as

$$\mathsf{L}_j(v,-u) = \begin{pmatrix} \alpha_1(v,-u)e_{11}^{(j)} + \beta(v,-u)\big[e_{22}^{(j)} + e_{33}^{(j)}\big] & \gamma_-(v,-u)e_{21}^{(j)} & \gamma_-(v,-u)e_{31}^{(j)} \\ \gamma_+(v,-u)e_{12}^{(j)} & \alpha_2(v,-u)e_{22}^{(j)} + \beta(v,-u)\big[e_{11}^{(j)} + e_{33}^{(j)}\big] & \gamma_-(v,-u)e_{32}^{(j)} \\ \gamma_+(v,-u)e_{13}^{(j)} & \gamma_+(v,-u)e_{23}^{(j)} & \alpha_3(v,-u)e_{33}^{(j)} + \beta(v,-u)\big[e_{11}^{(j)} + e_{22}^{(j)}\big] \end{pmatrix}, \tag{39}$$

$$\tilde{\mathsf{L}}_j(u,v) = \begin{pmatrix} \alpha_1(u,v)e_{11}^{(j)} + \beta(u,v)\big[e_{22}^{(j)} + e_{33}^{(j)}\big] & \gamma_+(u,v)e_{12}^{(j)} & \gamma_+(u,v)e_{13}^{(j)} \\ \gamma_-(u,v)e_{21}^{(j)} & \alpha_2(u,v)e_{22}^{(j)} + \beta(u,v)\big[e_{11}^{(j)} + e_{33}^{(j)}\big] & \gamma_+(u,v)e_{23}^{(j)} \\ \gamma_-(u,v)e_{31}^{(j)} & \gamma_-(u,v)e_{32}^{(j)} & \alpha_3(u,v)e_{33}^{(j)} + \beta(u,v)\big[e_{11}^{(j)} + e_{22}^{(j)}\big] \end{pmatrix} \tag{40}$$

with $e_{ab}^{(j)}$ a canonical basis of operators acting on $(\mathbb{C}^3)^{\otimes N}$. The monodromy matrix of the QTM, which provides another representation of the Yang-Baxter algebra (32), is given by

$$\mathsf{T}^{\mathrm{QTM}}(v) = \mathsf{L}_N(v,-u)\tilde{\mathsf{L}}_{N-1}(u,v)\ldots\mathsf{L}_2(v,-u)\tilde{\mathsf{L}}_1(u,v). \tag{41}$$

Using the representations (39) and (40) we can see that

$$|\Omega\rangle = \underbrace{\begin{pmatrix}1\\0\\0\end{pmatrix} \otimes \begin{pmatrix}0\\0\\1\end{pmatrix} \otimes \cdots \otimes \begin{pmatrix}1\\0\\0\end{pmatrix} \otimes \begin{pmatrix}0\\0\\1\end{pmatrix}}_{N\ \text{factors}} \tag{42}$$

is a pseudovacuum and

$$\mathsf{T}^{\mathrm{QTM}}(v)|\Omega\rangle = \begin{pmatrix} T_{11}^{\mathrm{QTM}}(v)|\Omega\rangle & T_{12}^{\mathrm{QTM}}(v)|\Omega\rangle & T_{13}^{\mathrm{QTM}}(v)|\Omega\rangle \\ T_{21}^{\mathrm{QTM}}(v)|\Omega\rangle & T_{22}^{\mathrm{QTM}}(v)|\Omega\rangle & T_{23}^{\mathrm{QTM}}(v)|\Omega\rangle \\ T_{31}^{\mathrm{QTM}}(v)|\Omega\rangle & T_{32}^{\mathrm{QTM}}(v)|\Omega\rangle & T_{33}^{\mathrm{QTM}}(v)|\Omega\rangle \end{pmatrix}$$
$$= \begin{pmatrix} [\alpha_1(v,-u)\beta(u,v)]^{N/2}|\Omega\rangle & T_{12}^{\mathrm{QTM}}(v)|\Omega\rangle & T_{13}^{\mathrm{QTM}}(v)|\Omega\rangle \\ 0 & [\beta(v,-u)\beta(u,v)]^{N/2}|\Omega\rangle & T_{23}^{\mathrm{QTM}}(v)|\Omega\rangle \\ 0 & 0 & [\beta(v,-u)\alpha_3(u,v)]^{N/2}|\Omega\rangle \end{pmatrix}.$$

The presence of the chemical potential term in the Hamiltonian (18) is taken into account via the transformation

$$\mathsf{T}^{\mathrm{QTM}}(v) \to \mathsf{T}^{\mathrm{QTM}}(v)\begin{pmatrix} e^{\beta h_1} & 0 & 0 \\ 0 & e^{\beta h_2} & 0 \\ 0 & 0 & e^{\beta h_3} \end{pmatrix}.$$

The QTM is defined as the trace in the auxiliary space of the monodromy matrix

$$\mathsf{t}^{\mathrm{QTM}}(v) = \mathrm{tr}_0\mathsf{T}^{\mathrm{QTM}}(v) = T_{11}^{\mathrm{QTM}}(v) + T_{22}^{\mathrm{QTM}}(v) + T_{33}^{\mathrm{QTM}}(v). \tag{43}$$

The existence of the pseudovacuum and the Yang-Baxter algebra (32) ensures that the eigenvalues of $\mathsf{t}^{\mathrm{QTM}}(v)$ for the grading $(---)$ can be obtained using ABA with the result (see Appendix A)

$$\Lambda^{\mathrm{QTM}}(v) = \lambda_1(v) + \lambda_2(v) + \lambda_3(v),$$

where

$$\lambda_1(v) = e^{\beta h_3}\left[\frac{\sin(\gamma - v - u)}{\sin\gamma}\frac{\sin(u - v)}{\sin\gamma}\right]^{N/2}\prod_{j=1}^{M}\frac{\sin\left(\gamma - v_j^{(1)} + v\right)}{\sin\left(v_j^{(1)} - v\right)},$$
$$\lambda_2(v) = e^{\beta h_1}\left[\frac{\sin(v + u)}{\sin\gamma}\frac{\sin(u - v)}{\sin\gamma}\right]^{N/2}\prod_{j=1}^{M}\frac{\sin\left(\gamma - v + v_j^{(1)}\right)}{\sin\left(v - v_j^{(1)}\right)}\prod_{i=1}^{M_1}\frac{\sin\left(\gamma - v_i^{(2)} + v\right)}{\sin\left(v_i^{(2)} - v\right)}, \tag{44}$$
$$\lambda_3(v) = e^{\beta h_2}\left[\frac{\sin(v + u)}{\sin\gamma}\frac{\sin(\gamma - u + v)}{\sin\gamma}\right]^{N/2}\prod_{j=1}^{M_1}\frac{\sin\left(\gamma - v + v_j^{(2)}\right)}{\sin\left(v - v_j^{(2)}\right)},$$

with $\{v_j^{(1)}\}_{j=1}^{M}$ ($\{v_i^{(2)}\}_{i=1}^{M_1}$) solutions of the BAEs $\lambda_1(v_j^{(1)})/\lambda_2(v_j^{(1)}) = -1$ [$\lambda_2(v_j^{(2)})/\lambda_3(v_j^{(2)}) = -1$].

VI. FREE ENERGY OF THE (− − −) PERK-SCHULTZ SPIN CHAIN

The free energy per lattice site of the Perk-Schultz spin chain is obtained from the largest eigenvalue of the QTM, denoted by $\Lambda_0(v)$, via the relation $f(h_1,h_2,h_3,\beta) = -\ln\Lambda_0(0)/\beta$. The largest eigenvalue lies in the $(N/2,N/2)$ sector which means that $M,M_1 = N/2$ in Eqs. (44). For our purposes, it is useful to change the spectral parameter $v \to iv$. Then, the expression for the largest eigenvalue can be written as ($N \in 4\mathbb{N}$)

$$\Lambda_0(v) = \lambda_1(v) + \lambda_2(v) + \lambda_3(v),$$
$$\lambda_j(v) = \phi_-(v)\phi_+(v)\frac{q_{j-1}(v + i\gamma)}{q_{j-1}(v)}\frac{q_j(v - i\gamma)}{q_j(v)}e^{\beta\tilde{h}_j}, \tag{45}$$

where $(\tilde{h}_1,\tilde{h}_2,\tilde{h}_3) = (h_3,h_1,h_2)$ and

$$\phi_\pm(v) = \left[\frac{\sinh(v \pm iu)}{\sin\gamma}\right]^{N/2},$$
$$q_j(v) = \begin{cases} \phi_-(v), & j = 0 \\ \prod_{r=1}^{N/2}\sinh\left(v - v_r^{(j)}\right), & j = 1,2 \\ \phi_+(v), & j = 3. \end{cases} \tag{46}$$

Using these notations, the Bethe equations can be written as $\lambda_j(v_r^{(j)})/\lambda_{j+1}(v_r^{(j)}) = -1$, $r = 1,\ldots,N/2$.

A. Nonlinear integral equations for the auxiliary functions

We want to obtain an integral expression for the largest eigenvalue of the QTM which can be easily implemented numerically. In this paper, we are going to use a method which can be understood as the multicomponent generalization of the technique presented in [84] (other thermodynamic descriptions of the Perk-Schultz spin chain can be found in [87–90]). We will introduce a set of two auxiliary functions for which the position of zeros and poles is known, allowing the derivation of NLIEs satisfied by these functions using the Cauchy theorem. In the last step, we are going to obtain an integral expression for the largest eigenvalue in terms of the auxiliary functions.

Define

$$\mathfrak{a}_1(v) = \frac{\lambda_1(v)}{\lambda_2(v)} = \frac{\phi_-(v + i\gamma)}{\phi_-(v)}\frac{q_1(v - i\gamma)}{q_1(v + i\gamma)}\frac{q_2(v)}{q_2(v - i\gamma)}e^{\beta(h_3 - h_1)}, \tag{47a}$$

$$\mathfrak{a}_2(v) = \frac{\lambda_3(v)}{\lambda_2(v)} = \frac{\phi_+(v - i\gamma)}{\phi_+(v)}\frac{q_1(v)}{q_1(v + i\gamma)}\frac{q_2(v + i\gamma)}{q_2(v - i\gamma)}e^{\beta(h_2 - h_1)}, \tag{47b}$$

with $\mathfrak{a}_j(v)$ periodic of period $i\pi$. Each of the equations $\mathfrak{a}_j(v) = -1$ has $3N/2$ solutions, of which $N/2$ are the Bethe roots $\{v_r^{(j)}\}_{r=1}^{N/2}$ and N solutions which are called holes and will be denoted by $\{v_r^{\prime(j)}\}_{r=1}^{N}$. The distribution of Bethe roots and holes characterizing the largest eigenvalue of the QTM for $\gamma \in (0,\pi/2)$ is presented in Fig. 8.

Let $\mathcal{C}$ be a rectangular contour with the upper (lower) edges parallel with the real axis through $\pm i(\gamma - \varepsilon)/2$, with $\varepsilon \to 0$ (please note that the contour is independent of N, the Trotter number). Inside the contour $\mathcal{C}$ the function $1 + \mathfrak{a}_1(v)$ [$1 + \mathfrak{a}_2(v)$] has $N/2$ zeros at the Bethe roots $\{v_r^{(1)}\}_{r=1}^{N/2}$ ($\{v_r^{(2)}\}_{r=1}^{N/2}$) and a pole of order $N/2$ at iu ($-iu$). Then, for v outside of the contour, and $j = \{1,2\}$ we can introduce

$$f_j(v) \equiv \frac{1}{2\pi i}\int_{\mathcal{C}}\frac{d}{dv}[\ln\sinh(v - w)]\ln[1 + \mathfrak{a}_j(w)]dw$$
$$= \frac{1}{2\pi i}\int_{\mathcal{C}}\ln\sinh(v - w)\frac{\mathfrak{a}_j'(w)}{1 + \mathfrak{a}_j(w)}dw, \tag{48}$$

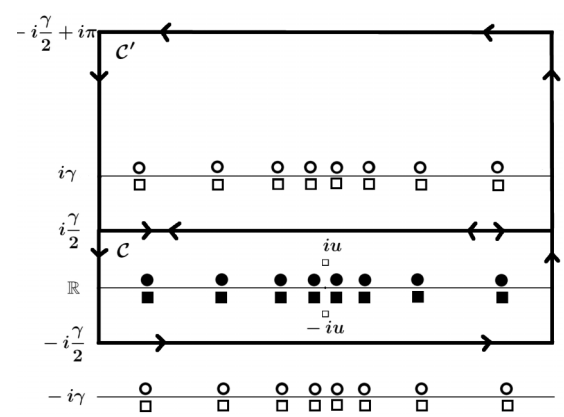

FIG. 8. Distribution of Bethe roots $\{v_i^{(1)}\}$, $\{v_j^{(2)}\}$ (●,■) and holes $\{v_i^{\prime(1)}\}$, $\{v_j^{\prime(2)}\}$ (○,□) characterizing the largest eigenvalue of the QTM [$\gamma \in (0,\pi/2)$]. The contour $\mathcal{C}$ contains all the Bethe roots and the poles of the auxiliary functions $\mathfrak{a}_j(v)$ at $\pm iu$. The lower edge of the contour $\mathcal{C}'$ (see Appendix B and next section) coincides with the upper edge of $\mathcal{C}$ but has opposite orientation.

where the right-hand side of (48) was obtained by taking into consideration that $\ln[1+\mathfrak{a}_j(v)]$ has no winding number due to the fact that the number of zeros inside the contour is equal to the order of the poles at $\pm iu$. We can evaluate $f_j(v)$ making use of the following theorem:

Theorem VI.1 [91]. Let $g(v)$ be an analytic function inside and on an arbitrary contour $\mathcal{C}$ in the complex plane. Let $\phi(v)$ be another function which is meromorphic inside and on the contour. Denoting the zeros of $\phi(v)$ in the interior of $\mathcal{C}$ by $a_1,a_2,\ldots$ (with multiplicities $r_1,r_2,\ldots$) and the poles by $b_1,b_2,\ldots$ (with multiplicities $s_1,s_2,\ldots$), then

$$\frac{1}{2\pi i}\int_{\mathcal{C}} g(v)\frac{\phi'(v)}{\phi(v)}dv = \sum_{i\in\text{ zeros}} r_i g(a_i) - \sum_{i\in\text{ poles}} s_i g(b_i),$$

with the result

$$f_1(v) = \ln q_1(v) - \ln\phi_-(v) - \frac{N}{2}\ln\sin\gamma, \tag{49a}$$

$$f_2(v) = \ln q_2(v) - \ln\phi_+(v) - \frac{N}{2}\ln\sin\gamma. \tag{49b}$$

Taking the logarithm of (47) and using (49) we find

$$\begin{aligned}\ln\mathfrak{a}_1(v) &= \beta(h_3-h_1)+\ln\left[\frac{\phi_-(v-i\gamma)}{\phi_+(v-i\gamma)}\frac{\phi_+(v)}{\phi_-(v)}\right]+f_1(v-i\gamma)\\ &\quad - f_1(v+i\gamma)+f_2(v)-f_2(v-i\gamma),\end{aligned} \tag{50a}$$

$$\begin{aligned}\ln\mathfrak{a}_2(v) &= \beta(h_2-h_1)+\ln\left[\frac{\phi_+(v+i\gamma)}{\phi_-(v+i\gamma)}\frac{\phi_-(v)}{\phi_+(v)}\right]+f_1(v)\\ &\quad - f_1(v+i\gamma)+f_2(v+i\gamma)-f_2(v-i\gamma).\end{aligned} \tag{50b}$$

Equations (50) are nonlinear integral equations of convolution type for $\mathfrak{a}_1(v)$ and $\mathfrak{a}_2(v)$ which are valid for all N. Using the identity

$$\lim_{N\to\infty}\ln\left[\frac{\phi_+(v)}{\phi_-(v)}\right] = i\beta J\sin\gamma\coth v,$$

we can perform the Trotter limit $N\to\infty$, obtaining

$$\begin{aligned}\ln\mathfrak{a}_1(v) &= \beta(h_3-h_1)-\beta\frac{J\sinh^2(i\gamma)}{\sinh v\sinh(v-i\gamma)}\\ &\quad+\int_{\mathcal{C}}K_0(v-w)\ln[1+\mathfrak{a}_1(w)]\,dw\\ &\quad-\int_{\mathcal{C}}K_2(v-w)\ln[1+\mathfrak{a}_2(w)]\,dw,\end{aligned} \tag{51a}$$

$$\begin{aligned}\ln\mathfrak{a}_2(v) &= \beta(h_2-h_1)-\beta\frac{J\sinh^2(i\gamma)}{\sinh v\sinh(v+i\gamma)}\\ &\quad+\int_{\mathcal{C}}K_1(v-w)\ln[1+\mathfrak{a}_1(w)]\,dw\\ &\quad-\int_{\mathcal{C}}K_0(v-w)\ln[1+\mathfrak{a}_2(w)]\,dw,\end{aligned} \tag{51b}$$

where

$$\begin{aligned}K_0(v) &= \frac{1}{2\pi i}\frac{\sinh(2i\gamma)}{\sinh(v+i\gamma)\sinh(v-i\gamma)},\\ K_1(v) &= \frac{1}{2\pi i}\frac{\sinh(i\gamma)}{\sinh(v+i\gamma)\sinh v},\\ K_2(v) &= \frac{1}{2\pi i}\frac{\sinh(i\gamma)}{\sinh(v-i\gamma)\sinh v}.\end{aligned} \tag{52}$$

Even though Eqs. (51) were derived assuming $\gamma\in(0,\pi/2)$, they remain valid also for $\gamma\in(\pi/2,\pi)$ by replacing $\mathcal{C}$ with a similar rectangular contour with the upper (lower) edges situated at $\pm i(\pi-\gamma-\varepsilon)/2$ with $\epsilon\to 0$. An observation is in order. The above results were derived assuming that v and $v\pm i\gamma$ were situated outside the contour $\mathcal{C}$. For v on the real axis, the integrands that appear in the definition of the functions $f_j(v)$ present an additional pole at v which means that in this case we have to add $\ln[1+\mathfrak{a}_2(v)]$ on the right-hand side of Eq. (51a) and $\ln[1+\mathfrak{a}_1(v)]$ on the right-hand side of Eq. (51b).

B. Integral expression for the largest eigenvalue

The free energy of the spin chain is obtained from the largest eigenvalue of the QTM evaluated at zero. Taking into account that $\Lambda_0(v)$ is analytical in a strip around the real axis then is sufficient to obtain an integral representation for $\Lambda_0(v_0)$ with v_0 inside the strip and then take the limit $v_0\to 0$. Choosing $v_0=-iu$, for which $\phi_+(v_0)=0$, and using (B1) we find

$$\Lambda_0(v_0) = c\,\frac{\phi_-(v_0)q_2^{(h)}(v_0)}{q_1(v_0)}. \tag{53}$$

Taking the logarithm of (53) and using (B5), we obtain (all constants are denoted by c)

$$\begin{aligned}\ln\Lambda_0(v_0) &= -\ln q_1(v_0)+\ln\phi_-(v_0)+\ln q_2^{(h)}(v_0)+c\\ &= \ln q_1^{(h)}(v_0)+\ln q_2^{(h)}(v_0)-\ln q_1(v_0+i\gamma)\\ &\quad-\ln q_2(v_0-i\gamma)-\ln[1+\mathfrak{a}_1(v_0)]+c\,.\end{aligned} \tag{54}$$

Now, we need integral representations for $\ln q_1^{(h)}(v_0)$ and $\ln q_2^{(h)}(v_0)$ with v_0 close to the real axis. For v inside the contour $\mathcal{C}$ consider

$$\begin{aligned}&\frac{1}{2\pi i}\int_{\mathcal{C}}d(v-w)\frac{\mathfrak{a}_1'(w)}{1+\mathfrak{a}_1(w)}dw\\ &\quad=-\frac{1}{2\pi i}\int_{\mathcal{C}'}d(v-w)\frac{\mathfrak{a}_1'(w)}{1+\mathfrak{a}_1(w)}dw,\end{aligned} \tag{55}$$

where on the right-hand side we have used (B4). The latter expression can be evaluated with the use of Theorem VI.1 and using that $1+\mathfrak{a}_1(v)$ is periodic of period $i\pi$ and inside the contour $\mathcal{C}'$ (see Appendix B) has N zeros which are holes $\{v_j'^{(1)}\}_{j=1}^N$ and N poles situated at $\{v_j^{(1)}-i\gamma\}_{j=1}^{N/2}$ and $\{v_j^{(2)}+i\gamma\}_{j=1}^{N/2}$ (some modulo $i\pi$). We find

$$\begin{aligned}\frac{1}{2\pi i}\int_{\mathcal{C}}d(v-w)\frac{\mathfrak{a}_1'(w)}{1+\mathfrak{a}_1(w)}dw &= -\sum_{j=1}^{N}d\big(v-v_j'^{(1)}\big)\\ &\quad+\sum_{j=1}^{N/2}d\big(v-v_j^{(1)}+i\gamma\big)+\sum_{j=1}^{N/2}d\big(v-v_j^{(2)}-i\gamma\big).\end{aligned} \tag{56}$$

For v inside the contour $\mathcal{C}$, $v+i\gamma$ is situated outside the contour. Then,

$$\frac{1}{2\pi i}\int_{\mathcal{C}} d(v-w+i\gamma)\frac{\mathfrak{a}_1'(w)}{1+\mathfrak{a}_1(w)}dw = \sum_{j=1}^{N/2} d\big(v-v_j^{(1)}+i\gamma\big) - Nd(v-iu+i\gamma)/2, \quad (57)$$

where we have used Theorem VI.1 and the fact that inside the contour the function $1+\mathfrak{a}_1(v)$ has $N/2$ zeros at the Bethe roots $\{v_j^{(1)}\}_{j=1}^{N/2}$ and a pole of order $N/2$ at iu. Taking the difference of (56) and (57), integrating by parts w.r.t w and then integrating everything w.r.t. v, we obtain

$$\frac{1}{2\pi i}\int_{\mathcal{C}}[d(v-w)-d(v-w+i\gamma)]\ln[1+\mathfrak{a}_1(w)]\,dw = \ln q_2(v-i\gamma) - \ln q_1^{(h)}(v) + \ln\phi_-(v+i\gamma) + c. \quad (58)$$

In an analogous fashion we find

$$\frac{1}{2\pi i}\int_{\mathcal{C}}[d(v-w)-d(v-w-i\gamma)]\ln[1+\mathfrak{a}_2(w)]\,dw = \ln q_1(v+i\gamma) - \ln q_2^{(h)}(v) + \ln\phi_+(v-i\gamma) + c. \quad (59)$$

Replacing $\ln q_1^{(h)}(v_0)$ and $\ln q_2^{(h)}(v_0)$ appearing in the second identity of (54) with the expressions which can be derived from (58) and (59) we find

$$\ln\Lambda_0(v_0) = \ln[\phi_+(v_0-i\gamma)\phi_-(v_0+i\gamma)] - \int_{\mathcal{C}} K_1(v_0-w) \times \ln[1+\mathfrak{a}_1(w)]\,dw + \int_{\mathcal{C}} K_2(v_0-w) \times \ln[1+\mathfrak{a}_2(w)]\,dw - \ln[1+\mathfrak{a}_1(v_0)] + c. \quad (60)$$

Equation (60) is in fact valid for v_0 in a narrow strip around the real axis as a consequence of the analyticity of the largest eigenvalue. Obtaining the constant of integration requires the introduction of

$$\bar{\Lambda}_0(v) = \frac{\Lambda_0(v)}{\phi_+(v-i\gamma)\phi_-(v+i\gamma)}, \quad (61)$$

which has the property of having constant asymptotics at infinity $\lim_{v\to\infty}\bar{\Lambda}_0(v) = e^{\beta h_1}+e^{\beta h_2}+e^{\beta h_3}$. All the previous considerations in this section are also valid for $\bar{\Lambda}_0(v)$ which means that

$$\ln\bar{\Lambda}_0(v) = c - \int_{\mathcal{C}} K_1(v-w)\ln[1+\mathfrak{a}_1(w)]\,dw + \int_{\mathcal{C}} K_2(v-w)\ln[1+\mathfrak{a}_2(w)]\,dw - \ln[1+\mathfrak{a}_1(v)], \quad (62)$$

with c a constant and v in a strip around the real axis. Taking the limit $v\to\infty$ and using $\lim_{v\to\infty}\mathfrak{a}_1(v) = e^{\beta(h_3-h_1)}$ and $\lim_{v\to\infty}\mathfrak{a}_2(v) = e^{\beta(h_2-h_1)}$, we find that

$$c = \ln\left[\frac{e^{\beta h_1}+e^{\beta h_2}+e^{\beta h_3}}{1+e^{\beta(h_2-h_1)}}\right] = \beta h_1 + \ln\left[\frac{1+e^{\beta(h_2-h_1)}+e^{\beta(h_3-h_1)}}{1+e^{\beta(h_2-h_1)}}\right]. \quad (63)$$

The last expression for the constant shows that in the scaling limit where $\beta = \bar{\beta}/\delta^2$ with $\delta\to O(\epsilon^2)$ and $h_1\to O(\epsilon^2)$, $h_{2,3}\to O(\epsilon^4)$ the term containing the square parentheses vanishes. Finally, from (61) and using $\lim_{v\to 0, N\to\infty}\ln[\phi_+(v-i\gamma)\phi_-(v+i\gamma)] = -J\beta\cos\gamma$, we obtain the integral expression for the largest eigenvalue

$$\ln\Lambda_0(0) = c - J\beta\cos\gamma - \int_{\mathcal{C}} K_2(w)\ln[1+\mathfrak{a}_1(w)]\,dw + \int_{\mathcal{C}} K_1(w)\ln[1+\mathfrak{a}_2(w)]\,dw - \ln[1+\mathfrak{a}_1(0)], \quad (64)$$

with c defined in (63). This expression, which was derived assuming $\gamma\in(0,\pi/2)$, remains valid also for $\gamma\in(\pi/2,\pi)$ by replacing $\mathcal{C}$ with a similar rectangular contour with the upper (lower) edges situated at $\pm i(\pi-\gamma-\varepsilon)/2$.

VII. CONTINUUM LIMIT

Having derived an integral expression for the free energy of the spin chain, all that remains in order to obtain the thermodynamic description of the 2CBG is to perform the continuum limit presented in Sec. IV. In the continuum limit, we can see from Table I that $\gamma = \pi-\varepsilon$ which means that the contour $\mathcal{C}$ appearing in Eqs. (51) and (64) has the upper (lower) edge parallel with the real axis situated at $\pm i(\pi-\gamma-\varepsilon)/2$. We will denote the upper edge of the contour situated at $i(\pi-\gamma)/2$ (the ε term is irrelevant for the following discussion) by $\mathcal{C}_+$ and by $\mathcal{C}_-$ the lower edge situated at $-i(\pi-\gamma)/2$. For $v\in\mathcal{C}_-$, $v = x-i(\pi-\gamma)/2$ with x real, the driving term in the right-hand side of (51a) is negative and equal with

$$\beta(h_3-h_1) - \beta\frac{J\sin^2\gamma}{\cosh(x+i\gamma/2)\cosh(x-i\gamma/2)}, \quad h_3<h_1,\ J>0$$

which means that in the scaling limit which implies $\beta\to\infty$, the auxiliary function $\mathfrak{a}_1(v)$ is very small on $\mathcal{C}_-$ and it can be neglected (for a rigorous justification see Ref. [92]). In a similar fashion, for $v\in\mathcal{C}_+$, $v = x+i(\pi-\gamma)/2$ with x real, the driving term in the right-hand side of (51b) is negative and equal with

$$\beta(h_2-h_1) - \beta\frac{J\sin^2\gamma}{\cosh(x+i\gamma/2)\cosh(x-i\gamma/2)}, \quad h_2<h_1,\ J>0$$

which means that the contribution of the auxiliary function $\mathfrak{a}_2(v)$ on $\mathcal{C}_+$ is also negligible. Therefore, in the scaling limit, Eqs. (51) take the form

$$\ln\mathfrak{a}_1(v) = \beta(h_3-h_1) - \beta\frac{J\sinh^2(i\gamma)}{\sinh v\sinh(v-i\gamma)} + \int_{\mathcal{C}_+} K_0(v-w)\ln[1+\mathfrak{a}_1(w)]\,dw - \int_{\mathcal{C}_-} K_2(v-w)\ln[1+\mathfrak{a}_2(w)]\,dw, \quad (65a)$$

$$\ln \mathfrak{a}_2(v) = \beta(h_2 - h_1) - \beta \frac{J \sinh^2(i\gamma)}{\sinh v \sinh(v + i\gamma)} + \int_{\mathcal{C}_+} K_1(v - w) \ln[1 + \mathfrak{a}_1(w)]\, dw - \int_{\mathcal{C}_-} K_0(v - w) \ln[1 + \mathfrak{a}_2(w)]\, dw. \tag{65b}$$

We can shift the free argument v and variable of integration to the line $+i\gamma/2$ for the function $\mathfrak{a}_1(v)$ and to the line $-i\gamma/2$ for the function $\mathfrak{a}_2(v)$ without crossing any poles of the driving terms obtaining

$$\ln \mathfrak{a}_1(v + i\gamma/2) = \beta(h_3 - h_1) - \beta \frac{J \sinh^2(i\gamma)}{\sinh(v + i\gamma/2) \sinh(v - i\gamma/2)} - \int_{\mathbb{R}} K_0(v - w) \ln[1 + \mathfrak{a}_1(w + i\gamma/2)]\, dw - \int_{\mathbb{R}} K_2(v - w + i\gamma - i\varepsilon) \ln[1 + \mathfrak{a}_2(w - i\gamma/2)]\, dw, \tag{66a}$$

$$\ln \mathfrak{a}_2(v - i\gamma/2) = \beta(h_2 - h_1) - \beta \frac{J \sinh^2(i\gamma)}{\sinh(v + i\gamma/2) \sinh(v - i\gamma/2)} - \int_{\mathbb{R}} K_1(v - w - i\gamma + i\varepsilon) \ln[1 + \mathfrak{a}_1(w + i\gamma/2)]\, dw - \int_{\mathbb{R}} K_0(v - w) \ln[1 + \mathfrak{a}_2(w - i\gamma/2)]\, dw, \tag{66b}$$

where we took into account the negative orientation of C_+. Performing similar transformations in the integral expression for the largest eigenvalue (64) we find

$$\ln \Lambda_0(0) = c - J\beta \cos\gamma + \int_{\mathbb{R}} K_2(w + i\gamma/2) \times \ln[1 + \mathfrak{a}_1(w + i\gamma/2)]\, dw + \int_{\mathbb{R}} K_1(w - i\gamma/2) \times \ln[1 + \mathfrak{a}_2(w - i\gamma/2)]\, dw - \ln[1 + \mathfrak{a}_1(0)]. \tag{67}$$

In the continuum limit, we have $\gamma = \pi - \epsilon$, $v \to \delta k/\epsilon$, $w \to \delta k'/\epsilon$ [we do not need the i factor because we have already considered the largest eigenvalue at iv, see the remark before (45)] and

$$K_0(v) \to -\frac{\epsilon}{\delta} \frac{1}{2\pi} \frac{2c}{k^2 + c^2}, \quad K_1(v - i\gamma) \to -\frac{\epsilon}{\delta} \frac{1}{2\pi} \frac{c}{k(k + ic)}, \quad K_2(v + i\gamma) \to -\frac{\epsilon}{\delta} \frac{1}{2\pi} \frac{c}{k(k - ic)}. \tag{68}$$

Introducing $a_1(k) = \mathfrak{a}_1(\delta k/\epsilon + i\gamma/2)$, $a_2(k) = \mathfrak{a}_2(\delta k/\epsilon - i\gamma/2)$ and taking the scaling limit in Eqs. (66), we obtain the NLIEs for the two-component Bose gas [Eqs. (7)].

The grand-canonical potential per unit length for the Bose gas is [see Eq. (24)] $\phi(\mu, H, \bar{\beta}) = [f(h_1, h_2, h_3, \beta) - E_0/L]/\delta^3$ with $f(h_1, h_2, h_3, \beta) = -\ln \Lambda_0(0)/\beta$ the free energy of the spin chain per lattice site and $E_0/L = J\cos\gamma - h_1$ the zero-point energy. In the continuum limit, the real part of the driving term on the right-hand side of Eq. (51a) becomes large and negative like $O(1/\epsilon^2)$, which means that $\ln[1 + \mathfrak{a}_1(0)]/\delta$ vanishes in this limit. Noticing that $K_1(\delta k/\epsilon - i\gamma/2) = K_2(\delta k/\epsilon + i\gamma/2) \sim \epsilon/2\pi$ with $dw = \delta dk/\epsilon$ and that the second term in the right-hand side of (63) vanishes in the same limit, we obtain Eq. (6) for the grand-canonical potential.

VIII. CONCLUSIONS

In this article, we have investigated the density profiles and local density correlation functions of the inhomogeneous 2CBG at finite temperature. Our results derived using a numerically efficient solution for the thermodynamics of the uniform system and the local density approximation predict that the polarization at the center of the trap has a significant influence on the local correlator throughout the sample, this effect becoming more pronounced at strong coupling. Even though our analysis of the density profiles did not find any evidence of phase separation, this scenario cannot be fully excluded in the region of low temperatures and small polarizations where our equations (and also the TBA result) become numerically unstable as a result of the first-order phase transition. The method employed in the derivation of the thermodynamics of the uniform system can also be used in the case of two-component fermions. In this case, the relevant lattice model is the $(-++)$ Perk-Schultz spin chain, and will be the subject of a future publication [93].

ACKNOWLEDGMENT

The research was funded by Volkswagen Foundation, Germany and the Romanian National Authority for Scientific Research (PNII-RU-TE-2012-3-0196).

APPENDIX A: ABA SOLUTION OF THE GENERALIZED $q = 3$ PERK-SCHULTZ MODEL

In this appendix, we present the solution of the generalized $q = 3$ Perk-Schultz model. The eigenvalues of the transfer matrix (33) and quantum transfer matrix (43) can be obtained as particular cases of this general solution. We should mention that the transfer matrix (33) was diagonalized in [61] and the eigenvalues of the quantum transfer matrix (43) were conjectured in [88]. For a proof of the results presented in the following, see Refs. [94–98].

The generalized $q = 3$ Perk-Schultz model is the set of all linear representations of the Yang-Baxter algebra

$$\check{\mathsf{R}}(v, w)[\mathsf{T}(v) \otimes \mathsf{T}(w)] = [\mathsf{T}(v) \otimes \mathsf{T}(w)]\check{\mathsf{R}}(v, w), \tag{A1}$$

with the R matrix defined in (25) and $\mathsf{T}(v)$ the monodromy matrix which acts triangularly on a pseudovacuum (highest vector) $|\Omega\rangle$:

$$\mathsf{T}(v)|\Omega\rangle = \begin{pmatrix} A(v)|\Omega\rangle & B_1(v)|\Omega\rangle & B_2(v)|\Omega\rangle \\ C_1(v)|\Omega\rangle & D_{11}(v)|\Omega\rangle & D_{12}(v)|\Omega\rangle \\ C_2(v)|\Omega\rangle & D_{21}(v)|\Omega\rangle & D_{22}(v)|\Omega\rangle \end{pmatrix} = \begin{pmatrix} \varphi_1(v)|\Omega\rangle & B_1(v)|\Omega\rangle & B_2(v)|\Omega\rangle \\ 0 & \varphi_2(v)|\Omega\rangle & D_{12}(v)|\Omega\rangle \\ 0 & 0 & \varphi_3(v)|\Omega\rangle \end{pmatrix}. \tag{A2}$$

The functions $\varphi_j(v)$, $j = 1,2,3$, are called the parameters of the model. The monodromy matrices of the transfer matrix (31) and QTM (41) satisfy these requirements with pseudovacua (35) and (42), respectively. The parameters of the model are given by

$$\varphi_1(v) = [\alpha_1(v,0)]^L, \;\; \varphi_2(v) = [\beta(v,0)]^L, \;\; \varphi_3(v) = [\beta(v,0)]^L \tag{A3}$$

in the transfer matrix case and by

$$\varphi_1(v) = e^{\beta h_1}[\alpha_1(v,-u)\beta(u,v)]^{N/2}, \; \varphi_2(v) = e^{\beta h_2}[\beta(v,-u)\beta(u,v)]^{N/2}, \; \varphi_3(v) = e^{\beta h_3}[\beta(v,-u)\alpha_3(u,v)]^{N/2} \tag{A4}$$

in the QTM case. The eigenvalues of the generalized model are [94,97,98]

$$\Lambda(v) = \varphi_1(v)\prod_{j=1}^{n} g_1\big(v_j^{(1)},v\big) + \varphi_2(v)\prod_{i=1}^{n} g_2\big(v,v_i^{(1)}\big)\prod_{j=1}^{m} g_2\big(v_j^{(2)},v\big) + \varphi_3(v)\prod_{j=1}^{m} g_3\big(v,v_j^{(2)}\big), \tag{A5}$$

with $\{v_i^{(1)}\}_{i=1}^n$, $\{v_j^{(2)}\}_{j=1}^m$ satisfying the BAEs $[g_i(v,w) = \alpha_i(v,w)/\beta(v,w)]$

$$\frac{\varphi_1\big(v_k^{(1)}\big)}{\varphi_2\big(v_k^{(1)}\big)} = \prod_{\substack{i=1\\ i\neq k}}^{n} \frac{g_2\big(v_k^{(1)},v_i^{(1)}\big)}{g_1\big(v_i^{(1)},v_k^{(1)}\big)}\prod_{j=1}^{m} g_2\big(v_j^{(2)},v_k^{(1)}\big), \quad k = 1,\ldots,n \tag{A6}$$

$$\frac{\varphi_2\big(v_l^{(2)}\big)}{\varphi_3\big(v_l^{(2)}\big)} = \prod_{i=1}^{n} g_2^{-1}\big(v_l^{(2)},v_i^{(1)}\big)\prod_{\substack{j=1\\ j\neq l}}^{m} \frac{g_3\big(v_l^{(2)},v_j^{(2)}\big)}{g_2\big(v_j^{(2)},v_l^{(2)}\big)}, \quad l = 1,\ldots,m. \tag{A7}$$

In the QTM case, it is preferable to work with a different pseudovacuum (see Ref. [94]) which amounts to cyclic permutations $(h_1,h_2,h_3) \to (h_3,h_1,h_2)$, $(\varepsilon_1,\varepsilon_2,\varepsilon_3) \to (\varepsilon_3,\varepsilon_1,\varepsilon_2)$ of the chemical potentials and grading in (A4). This explains the order of the chemical potentials in Eqs. (44).

APPENDIX B: PROOF OF SOME IDENTITIES

In this appendix, we prove several identities which we use in Sec. VI B. First, we will show that

$$\lambda_2(v) + \lambda_3(v) = c\,\frac{\phi_-(v)q_2^{(h)}(v)}{q_1(v)}, \quad q_2^{(h)}(v) = \prod_{j=1}^{N}\sinh\big(v - v_j^{\prime(2)}\big), \tag{B1}$$

with c a constant and $\{v_j^{\prime(2)}\}_{j=1}^N$ the holes corresponding to the equation $\mathfrak{a}_2(v) = -1$. Using (45) we have

$$\lambda_2(v) + \lambda_3(v) = \frac{\phi_-(v)}{q_1(v)}\frac{p_2(v)}{q_2(v)}, \tag{B2}$$

with $p_2(v) = \phi_+(v)q_1(v+i\gamma)q_2(v-i\gamma)e^{\beta h_1} + \phi_+(v-i\gamma)q_1(v)q_2(v+i\gamma)e^{\beta h_2}$. The function $p_2(v)$ has the following properties: $p_2(v+i\pi) = (-1)^{3N/2}p_2(v)$ and $\lim_{v\to\infty} p_2(v)/(\sinh v)^{3N/2} = \text{const}$. In addition, the equation $p_2(v) = 0$ is equivalent with $\mathfrak{a}_2(v) = -1$, which means that the zeros of $p_2(v)$ are the $N/2$ Bethe roots and the N holes. This shows that

$$p_2(v) = c\prod_{j=1}^{N/2}\sinh\big(v - v_j^{(2)}\big)\prod_{j=1}^{N}\sinh\big(v - v_j^{\prime(2)}\big) = c\,q_2(v)q_2^{(h)}(v),$$

which together with (B2) proves (B1). A similar reasoning can be applied to show

$$\lambda_1(v) + \lambda_2(v) = c\,\frac{\phi_+(v)q_1^{(h)}(v)}{q_2(v)}, \quad q_1^{(h)}(v) = \prod_{j=1}^{N}\sinh\big(v - v_j^{\prime(1)}\big), \tag{B3}$$

where $\{v_j^{\prime(1)}\}_{j=1}^N$ are the holes corresponding to the equation $\mathfrak{a}_1(v) = -1$.

Consider again the regime $\gamma \in (0,\pi/2)$ for which the distribution of roots and holes is presented in Fig. 8. The second useful result which we will prove is

$$\int_{\mathcal{C}+\mathcal{C}'} d(v-w)\frac{\mathfrak{a}_j'(w)}{1+\mathfrak{a}_j(w)}dw = 0, \quad d(v-w) = \frac{d}{dv}\ln\sinh(v-w), \tag{B4}$$

where $\mathcal{C}'$ (see Fig. 8) is a rectangular contour with the lower (upper) edges parallel to the real axis through $i(\gamma-\varepsilon)/2$ and $-i(\gamma-\varepsilon)/2+i\pi$ with $\varepsilon\to 0$. The lower edge of the contour $\mathcal{C}'$ at $i(\gamma-\varepsilon)/2$ coincides with the upper edge of $\mathcal{C}$ but has opposite orientation which means that the contribution of the $i\pi$-periodic integrand to the integral is zero. Then, relation (B4) is proved by noticing that the contributions of the sides parallel to the imaginary axis are also zero as a result of $\lim_{\mathrm{Re}w\to\pm\infty} d(v-w)=\mp 1$ and

$$\frac{\mathfrak{a}_j'(w)}{1+\mathfrak{a}_j(w)}=\frac{\mathfrak{a}_j'(w)}{\mathfrak{a}_j(w)}\frac{1}{1+\mathfrak{a}_j^{-1}(w)},$$

$$\lim_{\mathrm{Re}w\to\pm\infty}\frac{1}{1+\mathfrak{a}_1^{-1}(w)}\to\frac{1}{1+e^{\beta(h_3-h_1)}},\quad \lim_{\mathrm{Re}w\to\pm\infty}\frac{1}{1+\mathfrak{a}_2^{-1}(w)}\to\frac{1}{1+e^{\beta(h_2-h_1)}},\quad \lim_{\mathrm{Re}w\to\pm\infty}\frac{\mathfrak{a}_j'(w)}{\mathfrak{a}_j(w)}=0.$$

Using (B1) and (B3) and the definition of the auxiliary functions (47), we can also easily derive the following identities:

$$-\ln\phi_-(v)+\ln q_1(v)-\ln q_1(v+i\gamma)-\ln q_2(v-i\gamma)+\ln q_1^{(h)}(v)-\ln[1+\mathfrak{a}_1(v)]+c_1=0, \tag{B5}$$

$$-\ln\phi_+(v)+\ln q_2(v)-\ln q_1(v+i\gamma)-\ln q_2(v-i\gamma)+\ln q_2^{(h)}(v)-\ln[1+\mathfrak{a}_2(v)]+c_2=0, \tag{B6}$$

with $c_{1,2}$ constants and arbitrary v.

[1] I. Bloch, J. Dalibard, and W. Zwerger, Rev. Mod. Phys. **80**, 885 (2008).
[2] M. A. Cazalilla, R. Citro, T. Giamarchi, E. Orignac, and M. Rigol, Rev. Mod. Phys. **83**, 1405 (2011).
[3] X.-W. Guan, M. T. Batchelor, and C. Lee, Rev. Mod. Phys. **85**, 1633 (2013).
[4] T. Giamarchi, *Quantum Physics in One Dimension* (Oxford University Press, Oxford, UK, 2004).
[5] V. V. Cheianov and M. B. Zvonarev, Phys. Rev. Lett. **92**, 176401 (2004).
[6] G. A. Fiete and L. Balents, Phys. Rev. Lett. **93**, 226401 (2004).
[7] G. A. Fiete, Rev. Mod. Phys. **79**, 801 (2007).
[8] S. Akhanjee and Y. Tserkovnyak, Phys. Rev. B **76**, 140408 (2007).
[9] K. A. Matveev and A. Furusaki, Phys. Rev. Lett. **101**, 170403 (2008).
[10] A. Kamenev and L. I. Glazman, Phys. Rev. A **80**, 011603(R) (2009).
[11] M. B. Zvonarev, V. V. Cheianov, and T. Giamarchi, Phys. Rev. Lett. **103**, 110401 (2009).
[12] H. Moritz, T. Stöferle, M. Köhl, and T. Esslinger, Phys. Rev. Lett. **91**, 250402 (2003).
[13] T. Kinoshita, T. Wenger, and D. S. Weiss, Science **305**, 1125 (2004).
[14] B. Paredes *et al.*, Nature (London) **429**, 277 (2004).
[15] B. Laburthe Tolra, K. M. O'Hara, J. H. Huckans, W. D. Phillips, S. L. Rolston, and J. V. Porto, Phys. Rev. Lett. **92**, 190401 (2004).
[16] L. Pollet, S. M. A. Rombouts, and P. J. H. Denteneer, Phys. Rev. Lett. **93**, 210401 (2004).
[17] A. H. van Amerongen, J. J. P. van Es, P. Wicke, K. V. Kheruntsyan, and N. J. van Druten, Phys. Rev. Lett. **100**, 090402 (2008).
[18] E. H. Lieb and W. Liniger, Phys. Rev. **130**, 1605 (1963).
[19] J. M. McGuirk, H. J. Lewandowski, D. M. Harber, T. Nikuni, J. E. Williams, and E. A. Cornell, Phys. Rev. Lett. **89**, 090402 (2002).
[20] M. Erhard, H. Schmaljohann, J. Kronjäger, K. Bongs, and K. Sengstock, Phys. Rev. A **69**, 032705 (2004).
[21] A. Widera, O. Mandel, M. Greiner, S. Kreim, T. W. Hänsch, and I. Bloch, Phys. Rev. Lett. **92**, 160406 (2004).
[22] J. M. Higbie, L. E. Sadler, S. Inouye, A. P. Chikkatur, S. R. Leslie, K. L. Moore, V. Savalli, and D. M. Stamper-Kurn, Phys. Rev. Lett. **95**, 050401 (2005).
[23] L. E. Sadler, J. M. Higbie, S. R. Leslie, M. Vengalattore, and D. M. Stamper-Kurn, Nature (London) **443**, 312 (2006).
[24] A. Widera, S. Trotzky, P. Cheinet, S. Folling, F. Gerbier, I. Bloch, V. Gritsev, M. D. Lukin, and E. Demler, Phys. Rev. Lett. **100**, 140401 (2008).
[25] Y.-A. Liao, A. S. C. Rittner, T. Paprotta, W. Li, G. B. Partridge, R. G. Hulet, S. K. Baur, and E. J. Mueller, Nature (London) **467**, 567 (2010).
[26] E. Lieb and D. Mattis, Phys. Rev. **125**, 164 (1962).
[27] A. Kleine, C. Kollath, I. P. McCulloch, T. Giamarchi, and U. Schollwöck, Phys. Rev. A **77**, 013607 (2008).
[28] E. Eisenberg and E. H. Lieb, Phys. Rev. Lett. **89**, 220403 (2002).
[29] K. Yang and Y.-Q. Li, Int. J. Mod. Phys. B **17**, 1027 (2003).
[30] C. N. Yang, Phys. Rev. Lett. **19**, 1312 (1967).
[31] M. Gaudin, Phys. Lett. A **24**, 55 (1967).
[32] B. Sutherland, Phys. Rev. Lett. **20**, 98 (1968).
[33] Y. Q. Li, S. J. Gu, Z. J. Ying, and U. Eckern, Europhys. Lett. **61**, 368 (2003).
[34] J. N. Fuchs, D. M. Gangardt, T. Keilmann, and G. V. Shlyapnikov, Phys. Rev. Lett. **95**, 150402 (2005).
[35] M. T. Batchelor, M. Bortz, X. W. Guan, and N. Oelkers, J. Stat. Mech. (2006) P03016.
[36] M. B. Zvonarev, V. V. Cheianov, and T. Giamarchi, Phys. Rev. Lett. **99**, 240404 (2007).
[37] M. B. Zvonarev, V. V. Cheianov, and T. Giamarchi, Phys. Rev. B **80**, 201102(R) (2009).
[38] Y. Hao and S. Chen, Phys. Rev. A **80**, 043608 (2009).
[39] Y. Hao and S. Chen, Eur. Phys. J. D **51**, 261 (2009).
[40] S. Zölner, H.-D. Meyer, and P. Schmelcher, Phys. Rev. A **78**, 013629 (2008).
[41] Y. Hao, Y. Zhang, X.-W. Guan, and Shu Chen, Phys. Rev. A **79**, 033607 (2009).

[42] M. Knap, C. J. M. Mathy, M. Ganahl, M. B. Zvonarev, and E. Demler, Phys. Rev. Lett. **112**, 015302 (2014).
[43] C. J. M. Mathy, M. B. Zvonarev, and E. Demler, Nat. Phys. **8**, 881 (2012)
[44] N. J. Robinson, J.-S. Caux, and R. M. Konik, arXiv:1506.03502.
[45] A. G. Izergin and A. G. Pronko, Nucl. Phys. B **520**, 594 (1998).
[46] V. V. Cheianov, H. Smith, and M. B. Zvonarev, Phys. Rev. A **71**, 033610 (2005).
[47] B. Pozsgay, W.-V. van G. Oei, and M. Kormos, J. Phys. A: Math. Theor. **45**, 465007 (2012).
[48] S. Belliard, S. Pakuliak, E. Ragoucy, and N. A. Slavnov, J. Stat. Mech. (2013) P04033; (2012) P10017.
[49] S. Pakuliak, E. Ragoucy, and N. A. Slavnov, Nucl. Phys. B **881**, 343 (2014); Theor. Math. Phys. **181**, 1566 (2014); Nucl. Phys. B **893**, 459 (2015); SIGMA **11**, 063 (2015); **11**, 064 (2015); J. Phys. A: Math. Theor. **48**, 435001 (2015).
[50] J.-S. Caux, P. Calabrese, and N. A. Slavnov, J. Stat. Mech. (2007) P01008.
[51] M. Panfil and J.-S. Caux, Phys. Rev. A **89**, 033605 (2014).
[52] C. N. Yang and C. P. Yang, J. Math. Phys. **10**, 1115 (1969).
[53] M. Takahashi, *Thermodynamics of One-Dimensional Solvable Models* (Cambridge University Press, Cambridge, UK, 1999).
[54] S. J. Gu, Y. Q. Li, Z. J. Ying, and X. A. Zhao, Int. J. Mod. Phys. **16**, 2137 (2002).
[55] X. W. Guan, M. T. Batchelor, and M. Takahashi, Phys. Rev. A **76**, 043617 (2007).
[56] J. S. Caux, A. Klauser, and J. van den Brink, Phys. Rev. A **80**, 061605 (2009).
[57] A. Klauser and J. S. Caux, Phys. Rev. A **84**, 033604 (2011).
[58] A. Seel, T. Bhattacharyya, F. Göhmann, and A. Klümper, J. Stat. Mech. (2007) P08030.
[59] J. H. H. Perk and C. L. Schultz, Phys. Lett. A **84**, 407 (1981).
[60] C. L. Schultz, Phys. A (Amsterdam) **122**, 71 (1983).
[61] O. Babelon, H. J. de Vega, and C.-M. Viallet, Nucl. Phys. B **200**, 266 (1982).
[62] H. J. de Vega, Int. J. Mod. Phys. A **4**, 2371 (1989).
[63] H. J. de Vega and E. Lopes, Phys. Rev. Lett. **67**, 489 (1991).
[64] E. Lopes, Nucl. Phys. B **370**, 636 (1992).
[65] M. Suzuki, Phys. Rev. B **31**, 2957 (1985).
[66] T. Koma, Prog. Theor. Phys. **78**, 1213 (1987).
[67] M. Suzuki and M. Inoue, Prog. Theor. Phys. **78**, 787 (1987).
[68] A. Klümper, Ann. Phys. **504**, 540 (1992).
[69] A. Klümper, Z. Phys. B: Condens. Matter **91**, 507 (1993).
[70] A. Klümper and O. I. Pâţu, Phys. Rev. A **84**, 051604(R) (2011).
[71] M. Olshanii, Phys. Rev. Lett. **81**, 938 (1998).
[72] T. Bergeman, M. G. Moore, and M. Olshanii, Phys. Rev. Lett. **91**, 163201 (2003).
[73] K. V. Kheruntsyan, D. M. Gangardt, P. D. Drummond, and G. V. Shlyapnikov, Phys. Rev. A **71**, 053615 (2005).
[74] I. Bouchoule. K. V. Kheruntsyan, and G. V. Shlyapnikov, Phys. Rev. A **75**, 031606(R) (2007).
[75] P. P. Kulish, Phys. D (Amsterdam) **3**, 246 (1981).
[76] P. P. Kulish and N. Yu. Reshetikhin, Zap. Nauchn. Sem. LOMI. **120**, 92 (1982) [J. Sov. Math. **34**, 1948 (1986)].
[77] N. A. Slavnov, Theor. Math. Phys. **183**, 800 (2015).
[78] Introducing a length scale l_0 via $c = mgl_0/\hbar^2$, the units of grand-canonical potential per length, temperature, chemical potential, and magnetic field are $\phi_0 = \hbar^2/(2ml_0^3)$, $T_0 = \hbar^2/(2ml_0^2k_B)$, and $\mu_0 = h_0 = \hbar^2/(2ml_0^2)$.
[79] A. Klümper, Eur. Phys. J. B **5**, 677 (1998).
[80] D. M. Gangardt and G. V. Shlyapnikov, Phys. Rev. Lett **90**, 010401 (2003).
[81] K. V. Kheruntsyan, D. M. Gangardt, P. D. Drummond, and G. V. Shlyapnikov, Phys. Rev. Lett **91**, 040403 (2003).
[82] V. E. Korepin, N. M. Bogoliubov, and A. G. Izergin, *Quantum Inverse Scattering Method and Correlation Functions* (Cambridge University Press, Cambridge, UK, 1993).
[83] L. D. Faddeev, in *Les Houches Session LXIV, Quantum Symmetries, 1995*, edited by A. Connes, K. Gawedzki, and J. Zinn-Justin (Elsevier, Amsterdam, 1998).
[84] A. Klümper, Lect. Notes Phys. **645**, 349 (2004).
[85] F. Göhmann, A. Klümper, and A. Seel, J. Phys. A: Math. Gen. **37**, 7625 (2004).
[86] F. Göhmann and J. Suzuki, in *New Trends in Quantum Integrable Systems*, edited by B. Feigin, M. Jimbo, and M. Okado (World Scientific, Singapore, 2010).
[87] P. Zinn-Justin, J. Phys. A: Math. Gen. **31**, 6747 (1998).
[88] A. Klümper, T. Wehner, and J. Zittartz, J. Phys. A: Math. Gen. **30**, 1897 (1997).
[89] Z. Tsuboi and M. Takahashi, J. Phys. Soc. Jpn. **74**, 898 (2005).
[90] Z. Tsuboi, Nucl. Phys. B **737**, 261 (2006).
[91] E. T. Whittaker and G. N. Watson, *A Course of Modern Analysis* (Cambridge University Press, Cambridge, 1927).
[92] M. Dugave, F. Göhmann, and K. K. Kozlowski, J. Stat. Mech. (2014) P04012.
[93] O. I. Pâţu and A. Klümper (unpublished).
[94] See Supplemental Material at http://link.aps.org/supplemental/10.1103/PhysRevA.92.043631 for brief description of the algebraic Bethe ansatz for the generalized $q = 3$ Perk-Schultz model.
[95] F. Göhmann, Nucl. Phys. B **620**, 501 (2002).
[96] F. Göhmann and A. Seel, J. Phys. A: Math. Gen. **37**, 2843 (2004).
[97] D. Arnaudon, N. Crampe, A. Doikou, L. Frappat, and E. Ragoucy, Ann. Henri Poincaré **7**, 1217 (2006).
[98] S. Belliard and E. Ragoucy, J. Phys. A: Math. Theor. **41**, 295202 (2008).